ISSN 2087-3840

WOOD RESEARCH Journal

Journal of Indonesian Wood Research Society

Volume 9, Number 1, April 2018

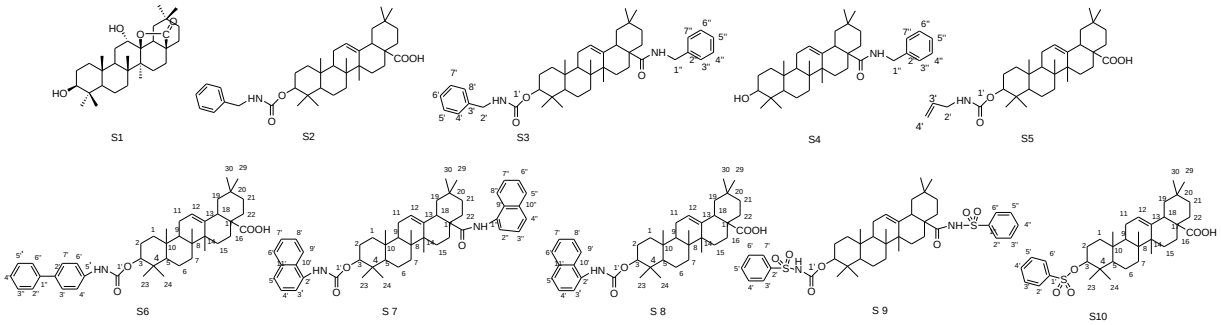

The Opportunities and Challenges of *Jati Plus Perhutani*	**Corryanti** and Novinci Muharyani	1
Correlation of the Areal Number Density of Vascular Bundles with the Mechanical Properties of Oil Palm Wood (*Elaeis guineensis* Jacq.)	**Rattana Choowang**	4
Heat Deflection Temperature (HDT) Properties of Polypropylene Composite Reinforced Cellulose Microfibrils of Oil Palm Empty Fruit Bunch and Frond	**Wida B. Kusumaningrum** and Sasa Sofyan Munawar	8
Pore Size Distribution and Microstructure of Oil Palm Shell Heat Treated at 300ºC Followed by Slow- or Fast Heating Treatment	**Joko Sulistyo**, Toshimitsu Hata, Yuji Imamura, Purnomo Darmadji, and Sri Nugroho Marsoem	15
Anti-proliferative Activity of Some Oleanolic Acid Derivatives with Potent Topoisomerase Inhibitory Activity on B16 Melanoma Cells	**Ahmed Ashour**, Ryuichiro Kondo and Kuniyoshi Shimizu	26

Volume 9, Number 1, April 2018 ISSN 2087-3840

WOOD RESEARCH Journal

Journal of Indonesian Wood Research Society

The Opportunities and Challenges of *Jati Plus Perhutani*

Corryanti and Novinci Muharyani

Abstract

The teak breeding program has long been conducted by Perum Perhutani and produced superior teak and was named Teak Plus of Perhutani - *Jati Plus Perhutani* (JPP). With good silviculture practices, JPP-teak of 9 year-old can produce no less than 100 m³/ha, with ± 60 cm of tree circumstance. The high demand for teak wood is an opportunity to develop JPP-teak with fast growing character. Research shows that the quality of JPP wood of 5 and 10 years of age can be classified into Strength Class III. Although the quality of JPP-teak is not equal as the teak gets older, it can be improved through several methods, such as densification, thermal modification, etc. Durability of fast growing JPP-teak can be enhanced by additional treatment with natural or chemical material preservation. Wood color modification can be done through heat treatment method. The color change of JPP-teak of 5 years of age that looked more brownies with variation in value of color change (ΔE*) of 1.04 to 48.53. Modification technology influenced the properties of teak wood and it is an opportunity of JPP to gain added value as a renewable forest resource product. With teak forest area covering 1.7 million hectares, Perum Perhutani has challenges in developing JPP-teak with more added value.

Keywords: JPP-teak, opportunity and challenges

Introduction

The utilization of teak wood for many purposes mainly because of its natural strength, durability, and beautiful fiber structure. Commercial teak wood usually comes from old teak wood with expensive material and finished product prices. Waiting until teak reaches the maximum age with good quality is assumed as inefficient today. Imbalance of supply and demand can not be avoided. Efforts to produce fast-growing teak is a solution to resolve the issue. However, the nature of this wood needs to be explored further and be compared to the quality of old teak. Perfomance of fast Fast growing performance teak wood coming with low wood quality is a challenge and interesting to be solved to correct the deficiencies.

JPP-Teak

The teak breeding in Perum Perhutani produces superior clones with fast growing character, known as JPP (Jati Plus Perhutani). The nine years old JPP-teak may produce timber not less than 100 m³/ha with 60 cm of mean circumference. Intensive silviculture practices (*silin*) on JPP-teak are expected in increasing the performance and productivity. It is mentioned in Basri and Wahyudi (2013) that the application of intensive silviculture can accelerate the heart wood formation and to gain straight stem. For further treatment, touch technology can improve the wood feature.

JPP teak-planting on a large scale was started since 2002 and now have reached not less than 200,000 hectares JPP plantation, spread over the Perum Perhutani forest area in Java. Results of studies on five and ten years old JPP wood (table1) classify JPP-teak into Strength Class-III. The visual observation on five years old JPP teak wood is white coloured dominant since it mostly consists of sapwood and secondary heart wood (Fig. 1-left). On the ten years old JPP teak, the heart wood percentages are between 45.80-55.95% varied on different sites.

Tabel 1. Some physical and mechanical feature of JPP-teak of 5 and 10 years old.

No	Parameters	Unit	JPP-wood	
			5 years old*	10 years old**
1	Specific gravity		0.56	0.55
2	Tangential shrinkage	%	4.2	3.59
3	Radial shrinkage	%	2.89	1.99
4	MOR	kg/cm^2	1001	858.37
5	MOE	1000 kg/cm^2	131.54	90.27
6	Strength class		III	III

Source Analyses result from Soil Laboratory, University of Gadjahmada Yogyakarta in Anonymous (2008) and Anonimous (2011).

Figure 1. Sampel of JPP teak wood of 5 years (left) and 10 years (right) old.

Efforts to improve the quality of JPP-teak require appropriate technology input to apply environmentally friendly principles to keep the sustainability of the forest (Anonymous 2013). This is in accordance to the sustainability principles adopted by Perum Perhutani in sustainable forest management (SFM). Sustainable forest management will be granted a certificate from the FSC, an independent organization recognized worldwide that supports sustainable forest management. The principles of sustainable forest management are mentioned as follows: (a) No timber harvesting or trading of illegal wood, (b) No violation to the rights of the traditional and human rights in forest management, (c) No damaging high conservation forest value, (d) No forest (natural) conversion to non-forest use, € No entering transgenic species in forest management, and (f) No violation to the ILO conventions (Anonymous 2013).

The Opportunity to Increase JPP-teak Quality and Utilization

Although many experts suggest cutting age of JPP–teak is at above 10 years (Basri and Wahyudi 2013) but in response to market demand, utilization of young wood with a touch of technology can be recommended. Quality improvement can be done through densification or impregnation. Tomme *et al*. (1998) in Hadiyane (2011) stated the main objective of these approaches are to improve the mechanical properties of the wood such as young's modulus, surface hardness, shear strength, and dimensional stability due to reduced portion of the cavity in wood (porosity) caused by compression. Hadiyane (2011) revealed that process of partial densification on Acacia and Agathis wood can improve physical and mechanical properties of wood, so wood would be more dense and hard, decreasing microfibril angle values and increasing the resistance to termite attack.

The use of heat treatment on five years old JPP using oven, steam, and autoclave at a temperature of 90, 120 and 150°C for 2 hours was effective to change the color of JPP wood (Muharyani 2012) and the greatest color change was gained by a steam method with total colour change value (ΔE *) of 44.85 (Muharyani *et al*. 2013) (Fig. 2).

Figure 2. The changing of JPP-teak colour after temperature treatment.

In increasing the utilization of JPP-teak, wood drying needs to be done. Basri and Wahyudi (2013) suggested JPP drying condition as follows: five year-old teak by using temperature of 30-40°C, seven year-old teak by using temperature of 40-50°C, and nine year-old teak by using temperature of 40-60°C. With 2.4 million ha of forest area, Perhutani has a wide-open challenge to increase the value of timber forest product. Differentiation of wood for a variety of different functions is an opportunity to be developed for JPP wood products. Wood as a lignocelulosic materials is a renewable resource and through the process of pyrolysis can be converted into high value products such as charcoal, activated carbon, carbon nano or carbon fiber (Pari 2010).

Conclusion and Recommendation

JPP-teak is the mainstay of Perhutani for it fast growing character. The opportunity to harvest JPP-teak within a young age with the right technology touch enable to utilize JPP-teak into a new product with a high added value that will give a positive impact on its uses for the people and the planet and also to the benefit of Perhutani as a company.

References

Anonymous. 2008. Analisis Kualita Kayu JPP umur 10 Tahun asal Tanaman Uji Keturunan. Puslitbang Perhutani. Cepu. Tidak dipublikasikan.

_____. 2011. Kajian Kualita Kayu Jati Plus Perhutani. Laporan Penelitian. Puslitbang Perhutani. Cepu. Tidak dipublikasikan.

_____. 2013. Penerapan Standard FSC Controlled Wood. Petunjuk Kerja. Perum Perhutani. Unit III Jawa Barat dan Banten. KPH Tasikmalaya.

Basri, E.; Wahyudi, I. 2013. Wood basic properties of Jati Plus Perhutani from different ages and their relationships to drying properties and qualities. Journal of Forest Products Research 31(2): 93-102.

Hadiyane, A. 2011. Perubahan Sifat-sifat Komponen Penyusunan Kayu, Struktur Sel Kayu dan Sifat-sifat Dasar Kayu Terdensifikasi Secara Parsial. Tesis. Sekolah Pascasarjana. Institut Pertanian Bogor. Bogor.

Muharyani, N. 2012. The Effect Of Temperature and Heat Treatment on Wood Properties of 5 Years Old Perhutani Superior Teak (*Jati Plus Perhutani*). Thesis. Faculty of Forestry. Universitas Gadjah Mada. Yogyakarta.

Muharyani, N.; Prayitno, T.A; and Widyorini, R. Steam Treated Jati plus Perhutani. Disampaikan pada 2nd INAFOR 2013. Dalam pengajuan pada Journal of Forestry Research.

Pari, G. 2010. Peran dan Masa Depan Arang yang Prospektif untuk Indonesia. Orasi Pengukuhan Profesor Riset Bidang kimia Kayu. Puslitbang Hasil Hutan. Balitbang Kehutanan. Kementerian Kehutanan.

Corryanti and Novinci Muharyani
Research and Development Center of Perum Perhutani
Jl Wonosari Batokan Tromol Pos 5 Cepu, Central Java, Indonesia
Email : corrysambodo@yahoo.com, novincimuharyani@yahoo.co.id

Correlation of the Areal Number Density of Vascular Bundles with the Mechanical Properties of Oil Palm Wood (*Elaeis guineensis* Jacq.)

Rattana Choowang

Abstract

Currently most of oil palm trunks in Thailand are left on the field to rot or are burnt in the field, not utilized as lumber. To promote such value-added uses, the objective of this study was to characterize the levels and variation within oil palm trunks of their key mechanical properties. In addition, the vascular bundle population was assessed, because this structural characteristic affected density and mechanical properties. The key ones being here were modulus of rupture (MOR), modulus of elasticity (MOE), and hardness. The 25 years old oil palm trunks were selected from a palm plantation in Surat Thani Province, in southern Thailand. The trees were cut down at 500 mm above ground, cut into dices, then sawn into small pieces in radial direction. Vascular bundle populations and basic densities were determined. Oil palm lumber was sawn from the logs between wood dices, and their mechanical properties were determined. The results indicated that the vascular bundle population density gradually decreased towards the central axis of trunks, and the population density positively correlated with basic density and mechanical properties. This was because the main component of a vascular bundle has fibers with thick cell walls. The data obtained may help select or create products that match the properties of oil palm wood (*Elaeis guineensis* Jacq.), or contributed to the sorting of wood raw material based on, for example, machine vision.

Keywords: oil palm wood, vascular bundle, basic density, mechanical property.

Introduction

Oil palm trees (*Elaeis guineensis* Jacq.) are important non-forest agricultural plants that may provide alternative raw material for the wood industries. In Thailand, oil palm plantation areas have expanded from 329,120 hectares in 2003 to 690,560 hectares in 2012, providing palm oil for food and renewable energy. More than 90% of total plantation area in Thailand is in its southern peninsular part, especially in Surat Thani, Krabi, and Chumphon provinces (Office of Agricultural Economics 2012). When the oil palm trees are past their economic life at 25 to 30 years old, the trunks are usually in the range of 15 to 18 meters in height and 45 to 60 centimeters in diameter. They are felled to make room for replanting, and normally left to rot or burnt down in the field (Katemanee 2006). Presently, oil palm trunks are not a raw material for wood industries, due to low density and poor mechanical properties compared to other commercial wood species from agro-forestry, such as rubberwood (Ratnasingam and Loras 2010). An oil palm trunk contains 31.70% to 47.30% cellulose, 21.20% to 34.40% hemicelluloses, and 18.40% to 29.60% lignin (Kaida *et al*. 2009; Yuliansyah *et al*. 2010; Chin *et al*. 2010; Verman and Saka 2011). The middle and core parts of trunk are 12.19% to 17.17% starch and it has high free sugar in sap (Yamada *et al*. 2010; Hashim *et al.* 2011). Especially in Thailand, these glucose based reserves in oil palm trunks have been studied for fermentation to produce bio-ethanol and hydrogen renewable energy (Punsuvon *et al*. 2005; Hniman *et al.* 2011). However, the oil palm wood taken from the bottom peripheral zone of stem can be used in furniture and in non-structural construction components (Ratnasingam and Loras 2010). Previous studies reported that the utilization of oil palm wood as lumber or laminated wood was difficult, because the product quality was affected by variation of physical and mechanical properties within trunk (Ratnasingam *et al*. 2008; Feng *et al*. 2011). The oil palm tree is a monocotyledon, and its main structure consists of vascular bundles embedded in parenchyma cells. The vascular bundles are the mechanical support and serve as a conduits for the transportation of water and nutrients in the trunk. Their number density per volume decreases towards the axial center, and increases in the trunk from the ground towards top of the tree (Erwinsyah 2008). Therefore, the objective of this study was to clarify the relation of vascular bundle population density with basic density and some mechanical properties of oil palm wood. The results may help rapidly estimate the mechanical properties of oil palm wood samples, and help with such selective use of oil palm wood that the quality control problems mentioned above are ameliorated.

Materials and Methods

Oil palm trees of 25 years of age were harvested from a local plantation in Surat Thani Province, in southern Thailand. The trees were cut down at 500 mm above ground, and cut into 60 mm thickness dices alternating with 1 m logs, as shown in Fig. 1. The oil palm dices were sawn into long pieces in the radial direction from pith to bark of trunk, 60 mm wide in tangential, and stored in plastic bags to avoid loss of moisture. The vascular bundle population density and the basic density were determined from these pieces. The logs between wood dices were sawn to lumber for mechanical property testing.

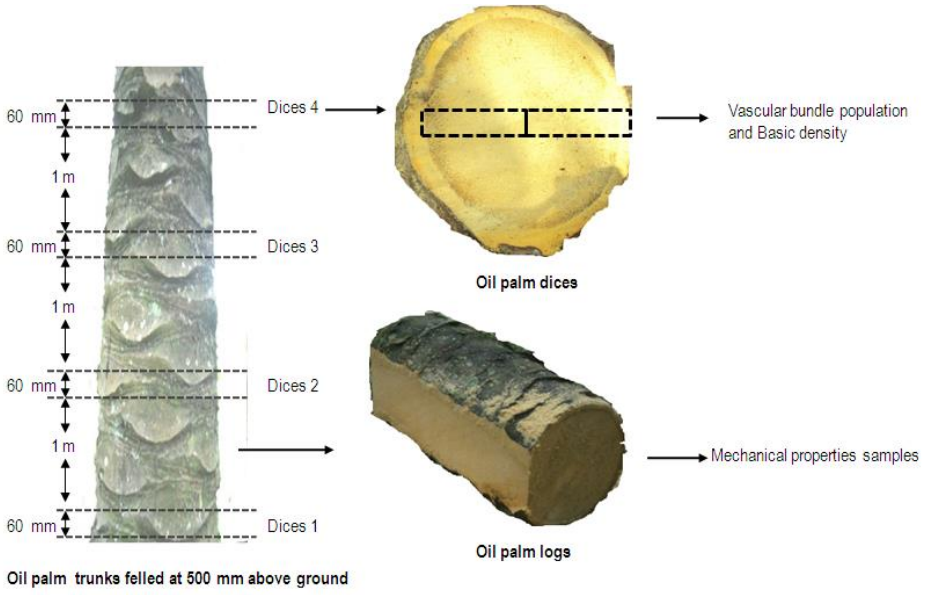

Figure 1. A schematic illustration of conversion of an oil palm trunk to the samples studied for vascular bundle population density, basic density, and mechanical properties.

The green oil palm woods which cut from dices were photographed from trunk axis to bark, using a stereo microscope, and the vascular bundles were counted from the images. Then, the same wood samples were cut to small 20 mm (tangential) x 20 mm (radial) x 25 mm (longitudinal) pieces to determine basic density profile, similarly from axis to bark. These green samples were measured in radial, tangential, and longitudinal directions with a digital caliper to the nearest 0.01 mm, weighed to nearest 0.01 g, and oven-dried at 103±2°C to constant weight. Finally, the oven-dry weights to the nearest 0.01 g were determined after cooling in desiccator. The basic density was calculated from the ratio of the oven-dry weight (g) and volume in green condition (cm^3).

Oil palm logs were sawn into 50 mm thick lumber using a polygon sawing pattern (Bakar *et al*. 2006), to separate the wood to inner, middle, and outer zones, that match the distribution of vascular bundles. The green lumber was air dried to a moisture content of 8-12%, and then planed and cut to 20 mm (tangential) x 20 mm (radial) x 300 mm (longitudinal) samples for static bending (modulus of rupture, MOR and modulus of elasticity, MOE), and to 20 mm (tangential) x 20 (radial) x 60 mm (longitudinal) samples for Janka type hardness test. All samples were conditioned in ambient 20°C temperature and 65% relative humidity until equilibrium moisture content, before the mechanical properties were determined using a universal testing machine. The testing of mechanical properties followed BS 373 standard (BS 373 1957) with slight modifications.

Results and Discussion

Microphotography of wood anatomy, using a stereo microscope, showed that the vascular bundles were unevenly distributed across the trunk, and surrounded by parenchyma cells. The population density increased radially from 23 Vp/cm^2 at the axial center to 115 Vp/cm^2 near bark, and varied by height along the trunk. The graph in Fig. 2 indicates a close relationship between this number density and basic density that increased from 0.11 g/cm^3 at the center to 0.40 g/cm^3 near bark. The vascular bundles were mostly fibers with thick cell walls, and this thickness was 8.08 µm at 2 m height. In addition, the thin walled parenchyma cells have a higher moisture content (Erwinsyah 2008; Fatimah *et al.* 2012). Therefore, the oven-dry weight of oil palm wood at high percentage of vascular bundles was high after they loosed the water in cell. This was the reason for the strong correlation with basic density.

The results in Fig. 3 showed that the overall mechanical properties of oil palm wood improve outwards from the axis. The average modulus of rupture, modulus of elasticity, and hardness of outer zone had the highest values at 26.20 MPa, 4861.49 MPa, and 1342.10 kg, respectively. Those properties were, in the same order, decreased to 8.76 MPa, 1711.39 MPa, and 486.10 kg for the middle zone, and further to 5.73 MPa, 516.53 MPa, and 223.60 kg for the inner zone. The areal number density of vascular bundles in the outer zone ranged from 68 Vp/cm^2 to 115 Vp/cm^2, and in the middle and inner zones from 44 Vp/cm^2 to 58 Vp/cm^2 and from 23 Vp/cm^2 to 40 Vp/cm^2, respectively.

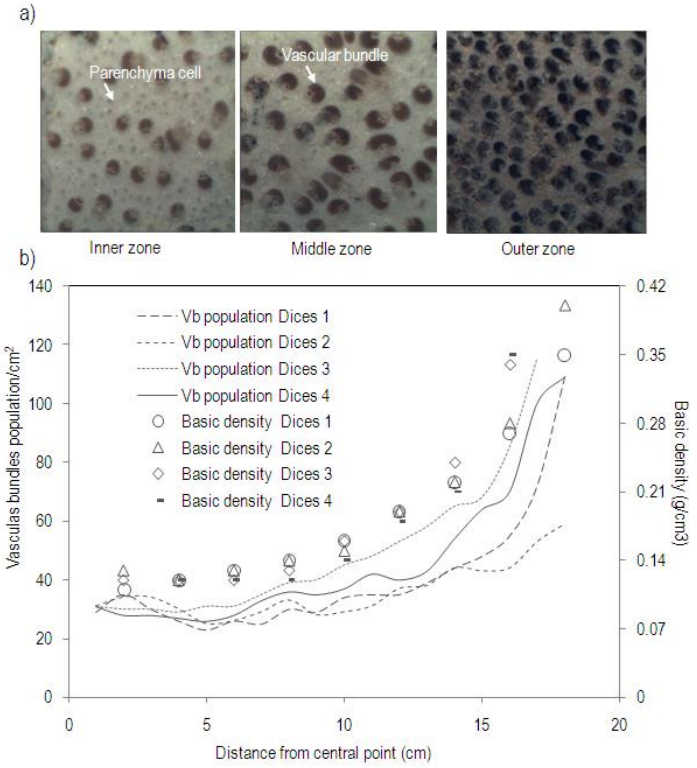

Figure 2. Microphotographs of inner, middle, and outer zones (a), and the relationship of radial profiles of vascular bundle density and basic density of oil palm wood, at various heights along the trunk (b).

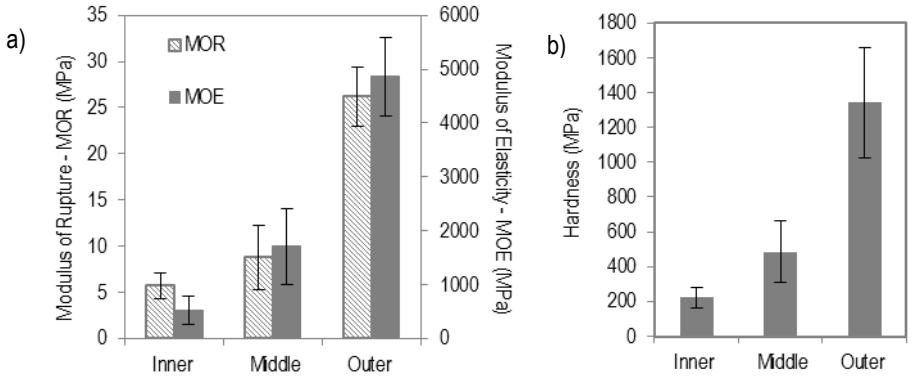

Figure 3. Modulus of rupture, Modulus of elasticity (a), and Hardness (b) of oil palm wood in inner, middle, and outer zones of the trunk.

Conclusions

The basic density and mechanical properties (static bending and hardness) of oil palm wood strongly correlated positively with the areal number density of vascular bundles. The data suggest that quick estimation of oil palm wood mechanical characteristics could be partly based on this areal number density. Such characterization could assist in rapid selection and avoiding destructive testing of the best parts of oil palm trunks for specific applications, for example by sorting based on machine vision.

Acknowledgments

The author is grateful for the support of Prince of Songkla University, Surat Thani Campus Research Fund. Assoc. Prof. Seppo Karrila, Ph.D. provided helpful comments on this manuscript.

References

Bakar, E.S.; F. Febrianto; I. Wahyudi; and Z. Ashari. 2006. Polygon Sawing: An Optimum Sawing Pattern for Oil Palm Stems. J Biol Sci. 6(4): 744-749.

British Standard. 1957. Methods of Testing Small Clear Specimens of Timber, BS 373, British Standards House, 2 Park ST., London, W.1

Chin, K.L.; P.S. H'ng; L.J. Wong; B.T. Tey; and M.T. Paridah. 2010. Optimization Study of Ethanolic Fermentation from Oil Palm Trunk, Rubberwood and Mixed Hardwood Hydrolysates using *Saccharomyces cervisian*. Biores Technol. 101: 3287-3291.

Erwinsyah V. 2008. Improvement of Oil Palm Wood Properties using Bioresin [PhD thesis]. Institit fur Forstntzung und Forsttechnik Fakultat fur Foest-,Geo- und Hydrowissenschaften: Technische Universitat Dresden.

Feng, L.Y.; P.M. Tahir; and Y.B. Hoong. 2011. Density Distribution of Oil Palm Stem Veneer and Its Influence on Plywood Mechanical Properties. J Appl Sci. 11(5): 824-831.

Hashim, R.; N. Said; J. Lamaming; M. Baskaran; O. Sulaiman; M. Sato; S. Hiziroglu; and T. Sugimoto. 2011. Influence of Press Temperature on the Properties of Binderless Particleboard Made from Oil Palm Trunk. Materials & Design 32: 2520-2525.

Hniman, A.; S. O-Thong; and P. Prasertsan. 2011. Developing a Thermophilic Hydrogen Producing Microconsortia from Geothermal Spring for Efficient Utilization of Xylose and Gucose Mixed Substrates and Oil Palm Trunk Hydrolysate. Int J Hydro Energy. 36: 8785-8793.

Katemanee, A. 2006. Appropriate Technology Evaluation for Oil Palm by Products Utilization in Krabi Province [M.S. thesis]. Faculty of Graduate Studies, Mahidol University 89 p.

Kaida, R.; T. Kaku; K. Baba; M. Oyadomari; T. Watanabe; S. Hartati; O. Sudarm; and Y. Hayashi. 2009. Emzymatic Saccharification and Ethanol Production of *Acacia mangium* and *Paraserianthes falcataria* Wood and *Elacis guineensis* Trunk. J Wood Sci. 55: 381-386.

Office of Agricultural Economic. 2012. Agricultural Statistics of Thailand. Bangkok, Thailand. 136 p.

Punsuvon, V.; W. Anpanurak; P. Vaithanomsat; and N. Tungkananurak. 2005. Fractionation of Chemical Components of Oil Palm Trunk by Steam Explosion. Proceeding of 31st Congress on Science and Technology of Thailand; 2005 October 18-20; Suranaree University of Technology.

Rarnasingam, J.; T.P. Ma; M. Manikam; and S.R. Farrokhpayam. 2008. Evaluating the Machining Characteristics of Oil Palm Lumber. Asian J. of Applied Sciences 1(4): 334-340.

Ratnasingam, J. and F. Loras. 2010. Static and Fatigue Strength of Oil Palm Wood Used in Furniture. J Appl Sci. 10(11): 986-990.

Sitti Fatimah, M.R.; O. Sulaiman; R. Hashim; T. Arai; A. Kosugi; H. Abe; Y. Murata; and Y. Mori. 2012. Characterization of Parenchyma and Vascular Bundle of Oil Palm Trunk as Function of Storage Time. Lignocellulose 1(1): 33-44.

Verman, M. and A.A. Saka. 2011. Comparative Study of Oil Palm and Japanese beech on their Fractionation and Characterization as Treated by Supercritical Water. Waste Biomass Valor. 2: 309-315.

Yamada, H.; R. Tanaka; O. Sulaiman; R. Hashim; Z.A.A. Hamid; M.K.A. Yahya; A. Kosugi; T. Arai; Y. Murata; S. Nirasawa; K. Yamamoto; S. Ohara; M.N.M. Yusuf; W.A. Ibrahim; and Y. Mori. 2010. Oil Palm Trunk: A Promising Source of Sugar for Bioethanol Production. Biomass & Bioenergy 34: 1608-1613.

Yuliansyah, A.T.; T. Hirajima; S. Kumagai; and K. Sasaki. 2010. Production of Solid Biofuel from Agricultural Wastes of the Palm Oil Industry by Hydrothermal Treatment. Waste Biomass Valor. 1: 395-405.

Rattana Choowang

Wood Sciences and Industry Technology Research Unit,
Faculty of Science and Industrial Technology,
Prince of Songkla University , Surat Thani Campus,
Mueang, Surat Thani 84000, Thailand.
E-mail : rattana.ch@psu.ac.th

Heat Deflection Temperature (HDT) Properties of Polypropylene Composite Reinforced Cellulose Microfibrils of Oil Palm Empty Fruit Bunch and Frond

Wida B. Kusumaningrum and Sasa Sofyan Munawar

Abstract

Polypropylene composites reinforcing with natural fiber is potentially applied for automotive particularly on interior part design. Those kind of composites were contributed on renewable material, rapid rate biodegradation, and low cost of production compared to synthetic fiber. Furthermore, the mechanical properties including strenghtness, young modulus, and thermal stability have revealed good performance than glass fiber. Fiber which were fibrillated and have high aspect ratio that coresspond to diameter and lenght ratio of the fiber were noticed as enhancement factor for mechanical properties. Fiber fibrillation processing into microfibrillated cellulose (MFC) attempts for widening surface area of the fiber that improve polymer matrices compatibility. MFC from empty fruit bunches (EFB) and oil palm frond (FB) fibers were performed as pulp by mechanically and chemically treatments. Chemically treatment was conducted with bleach and unbleach procedure. Polypropylene with fiber was mixed using kneader, and injection for molding process. Manufacturing uses needs appropriate size presition, moderate lead time, and low defect. Heat deflection temperature (HDT) provide information for plastic material on indicating temperature condition effect to material deformation during normal loading. Material of origin, additive or filler size, and molding temperature were directly corelated to the HDT performance. Initial temperature of HDT exhibits different value for different kind of fillers and fiber treatments. PP/EFB composite by mechanical treatment gives high value of HDT compared to the fiber processing by chemical treatment both with bleach and unbleach process. Similar result have been performed in PP/FB composites related to initial temperature. PP/ EFB composite with 30% of fiber loading represent HDT in 149.4°C, and for PP/ FB composite with 30% fiber loading gives 150.7°C. By the addition of fiber loading could improve the HDT value of the composites.

Keywords: oil palm empty fruit bunches , frond, polypropylene composite, HDT.

Introduction

Over the demand of sustainable and renewable material in several field such as automotive, medical, and food packaging, hence natural based material widely investigated in last decade. Natural fiber utillization for reinforcement material in polymer matrices especially in automotive part besides reduce the synthetic and metal material consumption that costly high but also could reduce total weight of cars which about 30% (Subyakto *et al*. 2009). Furthermore, by the natural fiber addition could overcome for green house effect since as an organic material, natural fiber could assist on carbon dioxide cycle (Hari 2012). Mostly in automotive manufacture remain use synthetic fiber and metal as main material. Synthetic fiber commonly used as reinforcement for plastic composites applied on interior part. The advantages of natural fiber related to renewable, biodegradable, good properties, low cost production (i.e. synthetic fiber), low density, non abrasive, relatively active surface, low carbon dioxide emission, and most of all as a green movement material (Zimmermann *et al*. 2004; Bhatnagar *et al*. 2005; Kamel 2007; Ashori 2008). Biocomposites is defined as material consisting of natural fiber as reinforcement and polymer as matric. Polymer usually used in automotive manufacture are provided from petroleum derivatives based such as Polypropylene and Polyethylene. Moreover by the addition of natural fiber, directly affect for polymer consumption reduction which better properties indeed. Molding process commonly used for automotive part are compression molding and extrusion followed with injection molding. However, the properties related such as mechanical, chemical, and thermal are disconnected for each molding process (Liu *et al*. 2007).

In common with wood, natural fibers have composition consist of cellulose, hemicellulose, and lignin. Secondary wall is imbeded by primary wall, in which cellulose mostly located. Cellulose is as crystalline part, while hemicellulose and lignin are amorphous part (Jonoobi *et al*. 2009). The depiction of composite are expressed in fibers that cellulose act as reinforce and the amorphous part (i.e. hemicellulose, lignin) role as matric. (Subyakto *et al*. 2009). Crystallinity of the cellulose are required in order to obtain high strength materials, so that some treatement are applied to degrade amorphous part particularly. Crystalline cellulose possesed 150 GPa in elastic modulus, higher than fiber glass (85 GPa) and aramid also (65 GPa) (Samir *et al*. 2004). Cellulose from non wood source could be an options such as flax, rutabaga, sisal, pineapple, coconut fiber, kenaf, and abaca (Bhatnagar *et al*. 2005) and also from alga, tunicate, and enzymatic isolation (Iwamoto *et al*. 2007).

Potencial lignocellulosic source especialy from industrial and agricultural or plantation waste is oil palm solid waste such empty fruit bunch (EFB) and palm frond (PF). According to the data oil palm plantation in Indonesia

reach 8.9 million hectar in 2011. The CPO production upgrading positively affect to increase oil palm solid waste. The potency are predicted 25 million tonne/ year for EFB and PF could achieve 89 million tonne /year. The utillization of EFB have been conducted with some kind of matrices such Polypropylene (PP), Polyvinyl chloride (PVC), Natural rubber, Phenol Formaldehide (PF), and Polyurethane (PU). Chemical modification was carried out in order to enhance compatibilty between fibers and polymer matric (Shinoj *et al*. 2011). Several researcher reported the uses of EFB for reinforcing agent to PP matric through out physical, chemical, and mechanical treatment (Sharkh *et al*. 2004; Khalid *et al*. 2008; Haque *et al*. 2009; Norul *et al*. 2013). Fiber composition strongly affected for mechanical properties of the composite (Khalid *et al*. 2008), similarly the surface modification with chemical treatment resulted strong hydrogen bonding between fibers and matrices (Haque *et al*. 2009; Norul *et al*. 2013). Norul *et al*. (2013), reported good resistance expose from PP/EFB composites including climate resistance and thermal stability under UV lightening.

Heat Deflection Temperature (HDT) is applied as an important parameter for material design. This property is used to decide appropriate processing technology particularly for high temperature manufacturing. HDT were applied to binary polymers and plastic composite for thermal property investigation since along time (Pava *et al*. 1974; Wong *et al*. 2003). Polymers having high degree of crystallinity with presence of fillers enhanced for HDT (Wong *et al*. 2003; Huda *et al*. 2006). Nano sized particle used for reinforcement or fillers could increase the HDT value even in small amount of fibers addition with well dispersion on matrices. (Thomas *et al*. 1996; Martins *et al*. 2009). Some factors that could enhance the HDT value were glass transition temperature, crystallinity, and fibers loading (Huda *et al*. 2006).

This research were aimed to investigate the HDT value from PP composites reinforced with empty fruit bunch and palm frond fibers. The effect of fibers composition both EFB and PF onto PP also analyzed toward to HDT value.

Experimental Methods

Materials

Polypropylene (PP) copolymer impact grade for automotive was used as the matric and Maleic anhydride Polypropylene (MAPP) was used as a coupling agent. Empty fruit bunch (EFB) and Palm frond (PF) were obtained from Subang, West Java. The fibers firstly processed with mechanical and chemical treatment before applied onto polymer matrices.

Mechanical and Chemical Pulp Preparation

The fibers by mechanical treatment were cuted using drum chipper, ring flaker, and hammer mill to obtain 0.5-1 cm of fibers. Further, obtained fibers were immersed in hot water with 100°C within 1 hour, ratio between water and fiber was determined at 1 : 10. Subsequently, treated fibers were milled with coarse disc refiner in 2 times, and finer in 5 times of circulation. Mechanical pulp were sieved with Jhonson screen, and kept under freez condition.

Kraft pulping process were carried out as the chemical treatement. 400 OD of cuted fibers were subjected onto NaOH (19% w/w) and Na2S (30% sulfidity) with krafting solution ratio larutan pemasak 5 : 1. Conditioned fibers were pulped using rotary digester under 160-170°C within 3.5 hours (lead time in 2 hours and processing time in 1.5 hours). Unbleached pulp were continously washed, refined, and filtrated with Jhonson screen. Whereas, bleached pulp were processed under C-E-H (Chlorinasion-Extraction-Hypochlorotation) methods. Chlorinasion step were conducted using Cl2 with 3.5% in consistency under 70°C in processing temperature. NaOH (1.5% w/w) were determined for extraction with 10% in consistency under 70°C within 90 minutes. Hypochlorotation were carried out with NaOCl (2% w/v) under 40 ° C within 240 minutes and 2% in consistency.

Production of Composites

Dried pulp were fibrillated using disc mill which have been dispersed in dry condition. PP were mixed with treated fiber (i.e. mehanical, unbleached pulp, bleached pulp) using kneader Daton under 160-170°C along 30-90 minutes of process. The mixed compound were milled with crusher to obtain uniform particle size and assist for feeding process. Then, were molded using injection molding (capacity 70 tonne) under injection condition at 230, 220, and 210°C respectively from feeder, and cooling time within 25 seconds. Resulted test piece were kept under vacuum bag to maintain the moisture content.

Heat Deflection Temperature Analysis

HDV 1 manual DTUL/ Vicat System ATLAS were subjected to analyzed the HDT value for all samples. The analysis based on ASTM D-648 technical test. The samples were placed edgewise with specimen dimension in 127 x 12.7 x 6.35 mm. Silicon oil GE SF 81-50, AK 1000 were used for heater medium under minimum flash temperature seted at 20°C above test temperature. Heating rate were determined in 2°C/minutes untill maksimum temperature reached 200°C. HDT value were noted as the sample undergo on deflection along 0.25 mm with normal loading.

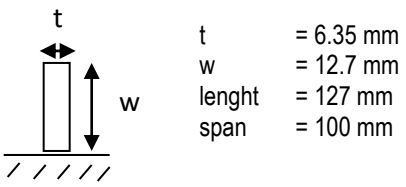

Figure 1. Configuration of HDT sample test.

Results and Discussion

Characterization of Composites

Cellulose content from EFB and PF relatively high. On PF fibers, cellulose content reach 62.34% and lignin 14.81% (Syamani *et al*. 2012). While cellulose content for EFB fibers is known in 41.72%, and other content such hemicellulose in 24.26%, lignin 22.49%, and extractive 11.54% (Anita *et al*. 2011). As depict on Fig. 2, that bleached pulp rather bright than unbleached pulp, while mechanical pulp almost like bleached pulp. Delignification and pulping process could enhance for cellulose content about 20.48%, 79.45%, and 85.4% respectively for mechanical pulp, unbleached pulp, and bleahced pulp, simultaneously lignin content reduce and significantly decrease for extractive content of EFB fibers (Kusumaningrum *et al*. 2012). Beside of cellulose crystallinity, -OH groups on cellulose gives strong hydrogen bonding with polymer matrices.

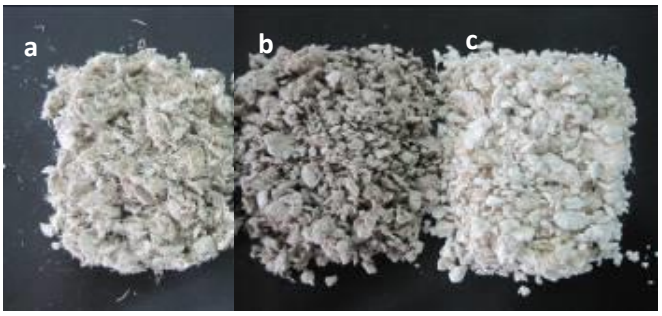

Figure 2. EFB pulp (a) mechanical pulp, (b) unbleached chemical pulp, (c) bleached chemical pulp.

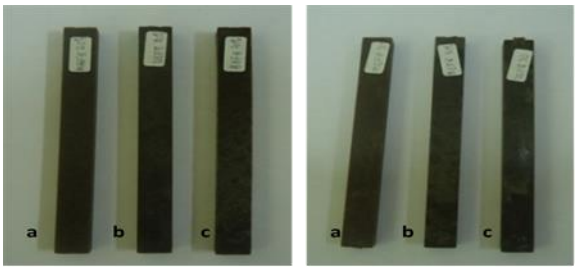

Figure 3. PP/EFB composites (a) mechanical pulp (EFB M), (b) unbleached pulp (EFB UB), (c) bleached pulp (EFB B) (Munawar *et al*. 2012).

Table 1. Composition of PP/EFB fibers composites and PP/PF fibers composites

Composites	Composition
EFB M 20	Mechanical EFB Fibers pulp 20%, PP 75%, MAPP 5%
EFB M 30	Mechanical EFB Fibers pulp 30%, PP 65%, MAPP 5%
EFB UB 20	Chemical Unbleached EFB Fibers pulp 20%, PP 75%, MAPP 5%
EFB UB 30	Chemical Unbleached EFB Fibers pulp 30%, PP 65%, MAPP 5%
EFB B 20	Chemical Bleached EFB Fibers pulp 20%, PP 75%, MAPP 5%
EFB B 30	Chemical Bleached EFB Fibers pulp 30%, PP 65%, MAPP 5%
PF M 20	Mechanical PF Fibers pulp 20%, PP 75%, MAPP 5%
PF M 30	Mechanical PF Fibers pulp 30%, PP 65%, MAPP 5%
PF UB 20	Chemical Unbleached PF Fibers pulp 20%, PP 75%, MAPP 5%
PF UB 30	Chemical Unbleached PF Fibers pulp 30%, PP 65%, MAPP 5%
PF B 20	Chemical Bleached PF Fibers pulp 20%, PP 75%, MAPP 5%
PF B 30	Chemical Bleached PF Fibers pulp 30%, PP 65%, MAPP 5%

Table 2. Density of PP/EFB and PP/PF composites.

Composites	Density (g/cm^3)
EFB M 20	0.942
EFB M 30	1.014
EFB UB 20	0.977
EFB UB 30	0.989
EFB B 20	0.976
EFB B 30	1.017
PF M 20	0.947
PF M 30	0.963
PF UB 20	0.978
PF UB 30	1.029
PF B 20	0.982
PF B 30	1.027

Composites composition between PP and EFB (PP/EFB) also PP and PF (PP/PF) with various fiber loading are given in Table 1. The opposite properties of PP and fibers which PP in hydrofobic and fibers in hydrofilic require MAPP as a coupling agent in order to improve polymer compatibilities onto fibers. According to previous study (Gopar *et al*. 2010), optimum MAPP loading in 5% (w/w) could increased the mechanical properties for PP reinforced with EFB fibers. Over limit MAPP could cause self entlangement that directly decrease the mechanical properties, similarly under limit MAPP could cause MAPP does not well grafted onto PP chain and further lacking of hydrogen bonding.

Composites feature from PP/EFB and PP/PS with mechanical and chemical pulp both unbleached and bleached are not significantly different particularly in colour appearance, as shown in Fig. 3. Some spot appeared in the composites surface, that probably created by greatly different of morphological and physiological properties between PP and fibers, because of gap, shear stress, and quenching during injection process. Table 2 is informed the enhancement of composites density by addition of EFB also PF fibers, even in slightly differences. Composites that reinforced with mechanical pulp gives lower density than chemical. It could be cause higher volume fraction of chemical pulp both unbleached and bleached after milling treatment using disc mill.

Heat Deflection Temperature (HDT) of PP/EFB and PP/PF Composites

HDT is widely used in material automotive industry and predicted some kind of problems related materials deformation. HDT value for PP/EFB composites are explained in Fig. 4, and Fig. 5 is revealed for PP/PF composites. The addition of EFB also PF fibers on PP matrices could enhance the HDT value. The HDT for pure PP were known at 113.6°C (Zhang *et al*. 2002) testing based on ASTM D 648 with deflection point at 0.25 mm under 1.82 Mpa loadings. Range about 8.71-32.66°C of HDT enhancement were obtain from PP/EFB, whereas 23.6-31.51°C from PP/PF composites. Presence of fibers could be as nucleating agent in crystalisation process, so that improve strenghtness and thermal stability of composites either PP/EFB and PP/PF and continously affected on HDT value enhancement. Huda *et al*. (2006) reported some parameters that influence HDT value of polymer, such crystalinity and reinforcement agent or filler. Kenaf fibers reinforcing onto PLA could improve the HDT value reaches 2 times than pure one in 40% fiber loading, because of spherulite formation during crsytalisation process (Huda *et al*. 2008).

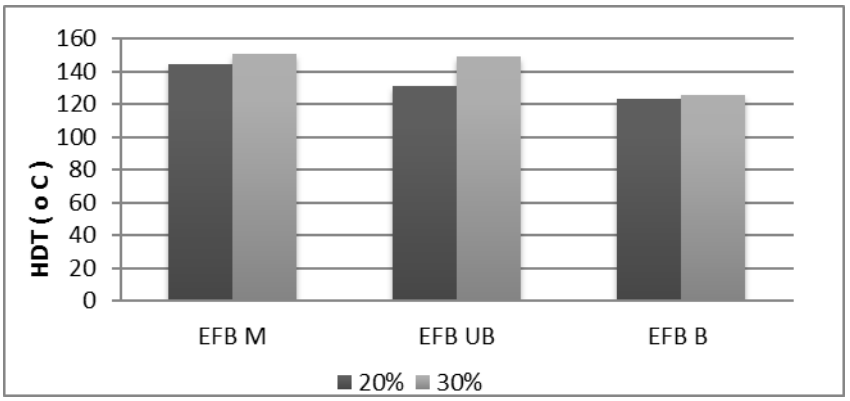

Figure 4. HDT value of PP/EFB composites for each treatment and fiber loading.

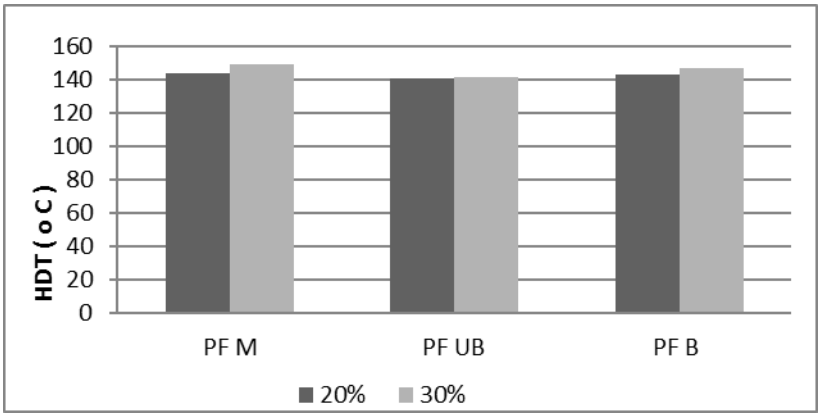

Figure 5. HDT value of PP/PF composites for each treatment and fiber loading.

Fiber loading in composite positively affect on HDT value. HDT value were increased with higher proportion of fiber loading for all kind of pulp, mechanical and chemical both for PP/EFB and PP/PF composites. HDT enhancement by fiber loading addition level result about 3.92%, 12.08%, and 1.59% respectively for mechanical pulp, chemical unbleached pulp, and bleached pulp for PP/EFB composite. While for PP/PF composites about 3.61%, 0.5%, and 2.72% respectively for mechanical pulp, chemical unbleached pulp, and bleached pulp. Fiber loading on CAP composites improved about 13 and 30% for composition under 15 and 30% (Mohanty *et al*. 2004). While, HDT value from PHBV/ wood flour composites increased 24°C through 40% in composition (Singh *et al*. 2007). As previous report at Huda *et al*. (2008), trancrystalinity spherulite formation were affected by nucleating agent quantity.

With optimum composition, presence of fibers could improve the strength and tensile modulus that corelated to HDT value. Pulping process of fibers were aimed for delignification in order to improve cellulose content that could refer to crsytallinity form. Beside that, could extensified suface contact with matrices because smaller particle size facilitate for hydrogen bonding that directly affect for mechanical and thermal properties. As reported before in Morreale *et al.* (2008) that finer particles having greater immobilisation ability on polymer chain. Previous study, Munawar *et al*. (2012) reported PP/EFB M having greater strength modulus achieved 45.51 MPa than PP/EFB UB and PP/EFB B. The result supported for corelation between strength modulus enhancement and HDT value improvement. As depicted from Figure 4 PP/EFB M have greater HDT value than PP/EFB UB and PP/EFB B. Similalry to PP/EFB, PP/PS M also have higher HDT value than PP/PF UB and PP/PF B. It could be fiber under milling process using disc mill caused lower aspect ratio of chemical pulp both unbleached and bleached due to horizontally cuted. Aspect ratio that correspond to lenght and width ratio of fibers significantly influence for plastic HDT value (Morreale *et al*. 2008). Some bubbles that were suspected as traped volatile chemical compound and water vapor, gradually create some cavity in composite reinfrocing chemical pulp as shown in Fig. 6. Nunez *et al*. (2002) adduced that volatile compound during heating process formed microcavity affected debonding between fiber and matrices.

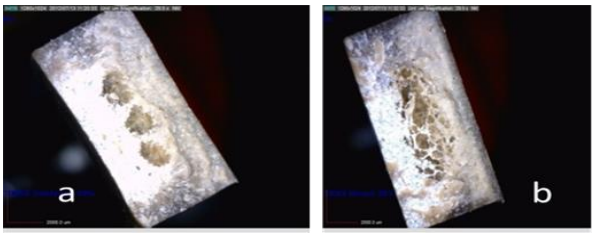

Figure 6. Microcavity on composite PP/EFB by chemical pulping, (a) EFB UB , (b) EFB B.

Conclusions

Heat deflection temperature of PP/EFB and PP/PF composites significantly improve by the addition of EFB and PF fibers with mechanical and chemical pulping. Composites reinforcing with mechanical pulp original from EFB (PP/EFB M) and PF (PP/PF M) have greater HDT value than reinfrocing with chemical pulp both unblecahed and bleached. Higher fiber loading relatively enhance for HDT value in all fibers treatment, mechanical pulp, chemical unbleached pulp, and chemical bleached pulp.

References

Abu Sharkh, B.F. and H. Hamid. 2004. Degradation Study of Date Palm Fibre/Polypropylene Composites in Natural and Artificial Weathering: Mecahnical and Thermal analysis. Polymer Degradation and Stability 85: 967-973.

Anita, S.H.; R. Lucky; E. Hermiati; and W. Fatriasari. 2011. Pretreatment of Oil Palm Empty Fruit Bunch (OPEFB) using Microwave Irradiation. In: Proceedings of the 3rd International Symposium of Indonesian Wood

Research Society. Jogjakarta, Indonesia, pp. 348-352.

Ashori, A. 2008. Wood Plastic Composites as Promising Green Composites for Automotive Industries. Bioresource Technolog.: 1-7.

Bhatnagar, A and M. Sain. 2005. Processing of Cellulose Nanofiber Reinforced Composites. Journal of Reinforced Plastic and Composites 24(12): 1259-1268.

Gopar, M.; Subyakto; K.W. Prasetiyo; and Ismadi. 2010. Karakteristik Biokomposit Plastik Mikrofibril Selulosa Tandan Kosong Kelapa Sawit. In: Proceedings of the 13th MAPEKI. Bali, Indonesia. pp. 86-92.

Hari. R.S. 2012. Teknik Manufaktur Komposit Hijau dan Aplikasinya. Performa 11(1): 9-18.

Haque, Md.M.; M. Hasan; M.S. Islam; and M.E. Ali. 2009. Phsyco-mechanical Properties of Chemically Treated Palm and Coir Fiber Reinforced Polypropylene Composites. Bioresource Technology 100: 4903-4906.

Huda, M.S; L.T. Drzal; A.K. Mohanty; and M. Misra. 2006. Chopped Glass and Recycled Newspaper as Reinforcement Fibers in Injection Molded PLA Composites: A Comparative Study. Composites Science and Technology 66: 1813-1824.

Huda, M.S.; L.T. Drzal; A.K. Mohanty; and M. Misra. 2008. Effect of Fiber Surface Treatments on the Properties of Laminated Biocomposites from PLA and Kenaf Fiber. Composites Science and Technology 68: 424-432.

Iwamoto, S.; A.N. Nakagaito; and H. Yano. 2007. Nanofibrillation of Pulp Fibers for the Processing of Transparent Nanocomposites. Applied Physical A. 89: 461-466.

Jonoobi, M.; J. Harun; A. Shakeri; M. Misra; and K. Oksman. 2009. Chemical Composition, Crytallinity, and Thermal Degradation of Bleached and Unbleached Kenaf Bast (*Hibiscus cannabinus*) Pulp and Nanofibers. Bioresources 4 (2): 626-639.

Kamel, S. 2007. Nanotechnology and Its Applications in Lignocellulosic Composites, a Mini Review. Express Polymer Letters 1(9): 546-575.

Khalid, M.; C.T. Ratnam; T.G. Chuah; S. Ali; Thomas; and S.Y. Choong. 2008. Comparative Study of Polyproylene Composites Reinforced with Oil Palm Empty Fruit Bunch Fiber and Oil Derived Cellulose. Materials and Design 29: 173-178.

Kusumaningrum, W.B.; S.M. Sasa; A. Lilik; K.H. Wawan K.H. 2012. Karakterisasi Kimia Pulp Tandan Kosong Kelapa Sawit. In: Proceedings of 2nd Masyarakat Perkelapasawitan Indonesia (MAKSI). Bogor, Indonesia. pp. 458-463

Liu, W.; L.T. Drzal; A.K. Mohanty; and M. Misra. 2007. Influence of Processing Methods and Fiber Length on Physical Properties of Kenaf Fiber Reinforced Soy Based Biocomposites. Composites Part B 38: 352-359.

Martins, C.G.; N.M. Larocca; D.R. Paul; and L.A. Pessan. 2009. Nanocomposites Formed from Polypropylene/ EVA Blends. Polymers 50: 1743-1754.

Mohanty, A.K.; A. Wibowo; M. Misra; and L.T. Drzal. 2004. Effect of Process Engineering on the Performance of Natural Fiber Reinforced Cellulose Acetate Biocomposites. Composites Part A 35: 363-370.

Morreale, M.; R. Scaffaro; A. Maio; F.P. La Mantia. 2008. Effect of Adding Wood Flour to the Physical Properties of Biodegradable Polymer. Composites Part A 39: 503-513.

Munawar, S.S.; B. Subiyanto; I. Budiman; L. Astari; and W.B. Kusumaningrum. 2012. Studi tentang Kekuatan Mekanis Komposit Polipropilena-Serat Tandan Kosong Sawit. Have been presented in MAPEKI XV, Makasar, Indonesia, 6 November 2012.

Norul, M.A.; M.T. Paridah; U.M.K. Anwar; M.Y. Mohd Nor; and P.S. H'ng. 2013. Effect of Fiber Treatment on Morphology, Tensile and Thermogravimetric Nanlysis of Oil Palm Empty Fruit Bunches Fibers. Composites Part B 45: 1251-1257.

Nunez, A.J.; M.K. Jose; M.R. Maria; I.A. Mirta; and E.M. Norma. 2002. Thermal and Dynamic Mechanical Characterization of Polypropylene - Woodflour Composites. Polymer Engineering and Science 42(4): 733-742.

Pava, A.; M. Rink; G. Blundo; and F. Danusso. 1974. Characterization of the Thermomechanical Behaviour of Polymers: Non-isothermal Creep Deflection Processes. Polymer 15: 243-247.

Samir M.; F. Alloin; M. Paillet; and A. Dufresne, Tangling. 2004. Effect in Fibrillated Cellulose Reinforced Nanocomposites. Macromoleculs 37: 4313-4316.

Shinoj, S.; R. Visvanathan; S. Panigrahi; and M. Kochubabu. 2011. Oil Palm Fiber (OPF) and Its Composites: A Review. Industrial Crops and Products 33: 7-22.

Singh, S. and A.K. Mohanty. 2007. Wood Fiber Reinforced Bacterial Bioplastic Composites: Fabrication and Performance Evaluation. Composites Science and Technology 67: 1753-1763.

Subyakto; E. Hermiati; D.H.Y. Yanto; Fitria; I. Budiman; Ismadi; N. Masruchin; and B. Subiyanto. 2009. Proses Pembuatan Serat Selulosa Berukuran Nano dari Sisal (*Agave sisalana*) dan Bambu Betung (*Dendrocalamus asper*). Berita Selulosa 44(2): 57-65.

Syamani, F.A. and B.K. Wida. 2012. Characteristic of Fibrillated Oil Palm Frond Pulp and Polyvinyl alcohol Composite, Have been presented in the 4th International Symposium of Indonesian Wood Research Society, Makasar, Indonesia, 7-8 November 2012.

Thomas, J.L. and W.M. Groenewoud. 1996. The Infulence of Fibre Length and Concentration on the Properties of Glass Fibre Reinforced Polyropylene: 2. Thermal Properties. Composites Part A, 27A: 555-565.

Wong, A.C. 2003. Heat Deflection Characteristics of Polypropylene/Polyethylene Binary System. Composites Part B, 34: 199-208.

Zhang, M.; Y. Liu; X. Zhang; J. Gao; F. Huang, Z. Song; G. Wei; and J. Qiao. 2002. The Effect of Elastomeric Nano Particles on the Mechanical Properties and Crystallization Behaviour of Polypropylene. Polymer 43: 5133-5138.

Zimmermann T.; E. Pohler; and T. Geiger. 2004. Cellulose Fibrils for Polymer Reinforcement. Advanced Engineering Materials 6(9): 754-761.

Wida B. Kusumaningrum and Sasa Sofyan Munawar
Research Center for Biomaterials LIPI,
Jl Raya Bogor Km 46 Cibinong Bogor
Email : wida.banar@biomaterial.lipi.go.id

Pore Size Distribution and Microstructure of Oil Palm Shell Heat Treated at 300ºC Followed by Slow- or Fast Heating Treatment

Joko Sulistyo, Toshimitsu Hata, Yuji Imamura, Purnomo Darmadji, and Sri Nugroho Marsoem

Abstract

Pore size distribution and microstructure development of oil palm shell heat treated at 300ºC and treated at 300ºC and recarbonization at 600ºC followed by slow- or fast heating treatment up to 700ºC were investigated by small angle X-ray scattering (SAXS), N_2 gas adsorption and Raman spectroscopy. On oil palm shell heat-treated at 300ºC, slow heating treatment gave the widening micropore along with the ordering microstructure; but fast heating treatment produced charcoal with a narrow diameter of micropore with wider pore size distribution and the disordering microstructure. On oil palm shell heat treated at 300ºC and recarbonization at 600ºC, slow heating treatment contributed on the opening new micropore with ordering microstructure, but some parts of micropore showing inaccessible for N_2 gas. Meanwhile, fast heating treatment with the heating rate from 75 to 250ºC/min increased BET surface area with similar pore size distribution and the disordering microstructure.

Keywords: Oil palm shell charcoal, pore size distribution, microstructure, slow- fast heating treatment, SAXS, Raman spectroscopy.

Introduction

Charcoal is carbonaceous material produced from carbonization process of biomass including wood and other biomass such as oil palm shell. The microstructure of charcoal consists of porosity which is the gaps between elementary graphitic crystallites and carbon skeleton which is formed by a graphitic sheet with a random orientation. The microstructure of charcoal from biomass is considered to provide an important contribution for the control in the development of biomass carbon based material (Ishimaru *et al.* 2007). In recent years, the microstructure of biomass based carbon has been used as the template for the formation of SiC, SiC/C and SiC/SiO_2/C composites (Greil 2001; Fujisawa *et al*. 2004; Vyshnyakova *et al*. 2006; Sulistyo *et al*. 2010). A detailed microstructural study of softwood pyrolysis performed by Paris *et al.* (2005) showed that the charring process commenced with the formation and growth of aromatic structures and nanopores at temperature higher than 327ºC. The ordering of the carbon structures occurred with the increase of heat treatment temperature from 400-800ºC (Yamauchi and Kurimoto 2003). This report had a good agreement with previous studies which defined that the formation microporosity system at 500ºC and used of the temperature range in the preparation of charcoal for activated carbons (Mackay and Roberts 1981; Pastor-Villegas *et al*. 1993; Lua *et al*. 2006). Carbonization at a temperature of 700ºC was conducted to prepare the charcoal for porous SiC ceramic (Fujisawa *et al*. 2004). Therefore, a condition of the carbonization especially temperature, obviously very much influence charcoal with the proper microstructure for production of carbon based materials.

Charcoal with a low degree of order of microstructure is generated from the production of smoke liquid from oil palm shell. The smoke liquid production is run at low temperature heat treatment of 300ºC to maximize the yield of liquid product and to minimize the content of polyaromatic hydrocarbons (Hattula *et al*. 2001; Demirbas 2001). A large amount of this solid waste charcoal material with high carbon content is potentially used as precursors for the preparation of adsorbents and for lignocellulosic ceramics such as SiC composites. However, the microstructure in the charcoal limits the further application and utilization. Until now, fewer studies have been reported on the utilization of the charcoal heat-treated at 300ºC.

Heat treatment of the solid waste charcoal oil palm shell was necessary to be carried out to improve a degree of the order of the microstructure in the material. The heat treatment of rockrose wood with a heating rate of 10ºC/min develops the charcoal with pores in the range of micro- to macropores (Pastor-Villegas *et al*. 1993). Heat treatment at a slow heating rate up to 800ºC removes volatile matters with a series of chemical reactions such as dehydration, breaking the C-O, C=O and C-C bonds, or repolymerization (Kurosaki *et al*. 2007). On the other hand, the fast heating with the rate of 6000ºC/min up to 800ºC made the chemical reactions occur concurrently and produced the charcoal with macroporous structure. In this study, the heat treatments with large different heating rates were carried out in order to produce the charcoal with different pore structures and microstructures from oil palm shell heat-treated at 300ºC. The pore size distribution and microstructure of oil palm shell heat-treated at 300ºC followed by slow-or fast heating treatments up to 700ºC were investigated by small angle X-ray scattering (SAXS) and Raman spectroscopy. The

effect of reaction times in slow heating treatment and that of heating rates in fast heating treatment were examined in this study.

Experimental

Heat Treatment

Air dried oil palm shell (OPS) with the characteristics as shown in Table 1 was heat-treated at a rate of 10ºC/min and was maintained constant at 300ºC for 180 min in an electric cylindrical steel furnace of 1 kg capacity. The charcoal heat-treated at 300ºC noted as HT1. The furnace was connected to a water-cooled condenser to entrap liquid by cooling smoke. After heat treatment, HT1 charcoals were granulated by a hammer mill to be sieved to 63-150 µm. As the comparison of the effect of heating at 600ºC, part of HT1 samples were re-carbonized up to 600ºC at 10ºC/min and were then held at this temperature for 60 min in a muffle furnace. The charcoal from the heat treatment at 300ºC and then followed by re-carbonization at 600ºC noted as HT2.

Slow Heating Treatment

Dry weight of 20 g of HT1 or HT2 charcoal was mixed with 40 ml distilled water containing 4 g of $ZnCl_2$ at 60ºC. The small amount of $ZnCl_2$ was used in the mixture to aid in porosity development in charcoal (Rodriguez-Reinoso and Molina-Sabio 1992). The dehydrated materials were dried at 115ºC for 3 h in an electric oven and then were heat-treated at 10 °C/min up to 700ºC, and then kept for 60, 120 and 180 min in a muffle furnace. After cooling, charcoals were washed with 0.1 N HCl and water and then were dried at 115ºC.

Fast Heating Treatment

Dry weight of 0.2 g of HT1 or HT2 charcoal was put into a 10 mm of the diameter of graphite die with a length of 5 cm (point 1 in Fig. 1) which was closed with two graphite punches (point 2 in Fig. 1) with a length of 2.5 and 2.2 cm. The charcoal in the graphite die was placed in a pulse current sintering apparatus (VCSP-II, SS-Alloy Co. Ltd., Hiroshima) as sketched in Fig. 1. The charcoal was heat-treated at 75, 250, 1000 and 2000ºC/min up to 700ºC and was kept for 15 min under N_2 gas flow with a rate of 100 mL/min. A pressure of 12 MPa on the graphite die which had minimum effects on the charcoal was applied from the start of the heating and was released after cooling.

Tabel 1. Proximate and ultimate analysis of raw and carbonized material oil palm shell.

Samples	Proximate and ultimate analysis (%, dry basis)						
	Volatile matter	Fixed carbon	Ash	C	H	N	$O_{diff.}$
OPS	73.08	13.30	2.37	49.64	6.76	0.20	41.03
HT1	22.31	36.52	5.69	77.95	2.05	0.22	14.09
HT2	10.81	69.73	6.45	89.39	2.44	0.16	1.56

Note: OPS is raw oil palm shell. HT1 charcoal is oil palm shell heat-treated at 300ºC for 180 min; HT2 charcoal is oil palm shell heat-treated at 300ºC for 180 min and then followed by re-carbonization at 600ºC for 60 min. $O_{diff.}$ is estimated by difference from 100-C-H-N- Ash elements.

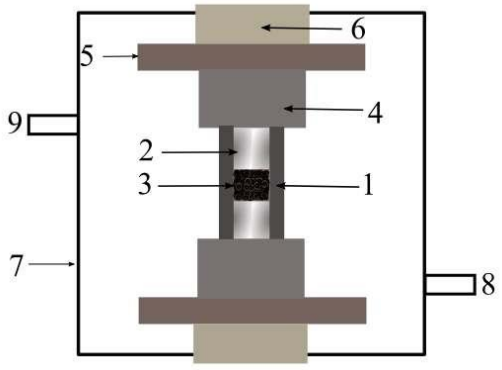

Figure 1. Schematic of a pulse current sintering apparatus. (1) Graphite die; (2) graphite punch; (3) sample; (4) graphite disc; (5) graphite plate; (6) copper electrode; (7) chamber; (8) vacuum pump; and (9) optical pyrometer.

Pore Distribution, Surface Area, and Microstructure Analysis

The pore size and distribution were analyzed by a three-slit optical systems with a line focus of SAXS (small-angle X-ray scattering, Rigaku Corporation, Japan). X-ray generator was operated at 50 kV and 200 mA. The intensity was measured with a scintillation counter. The scattered intensity was recorded as a function of the scattering wave vector,

$$q = \frac{4\pi}{\lambda}\sin\frac{\theta}{2} \quad (1)$$

where λ is the X-ray wavelength and 2θ is the scattering angle. The scattered intensity of charcoal which was put into a transparent capiller (Borokapillaren glas, Germany) with a diameter of 1 mm and a length of 80 mm was corrected by that of the transparent capiller without charcoal.

The pore size distribution was analyzed by using NANO-Solver Ver. 3.4 (Rigaku Corporation, Japan). This software program conducted profile fittings over the entire measurement range of scattered intensity in order to improve reproducibility in analysis. Least-squares methods were adopted to optimize the fitting parameters for a spherical model, assuming dispersed spheres. The spherical model which was fitted to the measurement data calculated the scattering intensity which depended on the form factor and structure factor using the following equation (Rigaku Corporation 2006):

$$I(q) = |F(q)|^2 S(q) \quad (2)$$

where *F(q)* is the form factor of the pore with a sphere shape possessing a radius R, and *S(q)* is the structure factor which is equal 1 when the pores are randomly distributed in the medium. The spherical model with a radius of R is used in the description of form factor (Rigaku Corporation 2006) as follow

$$F(q, D) = \Delta\rho \frac{4\pi}{q^3}\left(\sin(qR) - qR\cos(qr)\right) \quad (3)$$

where $\Delta\rho$ is electron density difference at position R. The structure factors are expressed by following equations (Rigaku Corporation 2006):

$$S(q) = 1 + \int_v \left(n(r) - n_0\right) e^{iq.r}\, dr \quad (4)$$

where n_0 is average particle density. The pore distribution assumes Γ distributions which are expressed by the following equation (Rigaku Corporation 2006)

$$P_{R_0}^M(R) = \frac{1}{\Gamma(M)}\left[\frac{M}{R_0}\right]^M e^{\frac{MR}{R_0}} R^{-1+M} \quad (5)$$

where R_0 is the average pore radius and *M* is the shape parameter in the software. The shape parameter *M* is expressed by σ, the normalized dispersion normalized by average size, as follows (Rigaku Corporation 2006):

$$\sigma = \frac{\sqrt{\delta R^2}}{R_0} x100 = \frac{1}{\sqrt{M}} x100 \quad (6)$$

The pore size of HT1 and HT2 charcoals was also analyzed by N_2 adsorption at 77 K by a NOVA 2000 (Quantachrome Instruments, USA). The pore size was determined by the Barret-Joyner-Halenda (BJH) models (Barrett *et al*. 1951). In the case, surface area using Brunauer-Emmett-Teller (BET) equation (Brunauer *et al*. 1938) and adsorption isotherm in HT2 charcoals prepared by slow- and fast heat treatment were determined from N_2 adsorption at 77 K by a TriStar II 3020 (Micromeretics Instrument Corporation, USA).

A Raman spectroscopy (Renishaw inVia, England) equipped with an air-cooled CCD detector was used to analyze the carbon microstructure of the charcoals. An argon laser (514.5 nm) was adopted as an excitation source. The laser was focused to approximately 1 μm in diameter at a power of less than 1 mW on the charcoal surface in order to prevent irreversible thermal degradation. Spectra were measured in the 1,100-1,800 cm^{-1} range. Six 10-second accumulations gave adequate signal-to-noise ratio of the spectra. The wave number was calibrated using the 520 cm^{-1} line of a silicon wafer. Spectral processing was performed using WiRE 2 software. The crystallite size or coherence length (L_a) was determined from Raman peak data by an empirical formula developed by Tuinstra and Koening (1970):

$$L_a = \frac{(43.5\,\text{Å})}{I_d / I_g} \quad (7)$$

Proximate and Ultimate Analysis

Proximate analysis, including moisture, ash content, and volatile matter, were determined by ASTM D 2867-70, D 2866-70, and D 1762-64, respectively (1970; 1977). The fixed carbon content was obtained by difference. Ultimate analyzes was carried out by Perkin Elmer elemental analyzer 2400. The oxygen content was obtained by difference. The proximate and ultimate analyses were conducted on oil palm shell, HT1, and HT2 charcoals.

Results and Discussion

Pore Size Distribution

Fig. 2 shows an example of pore distribution analysis of a SAXS profile of HT2 charcoal by NANO-Solver, which was calculated by a curve fitting method where a simulated curve was to be fitted to a SAXS profile from scattering. In the SAXS profile, the scattering intensity in the low and high degree regions of 2θ attributed to inter- and intraparticle disorder, corresponding to meso- and micropore, respectively. The curve fitting analysis showed that the dominant pore structures of HT2 charcoal were micropores.

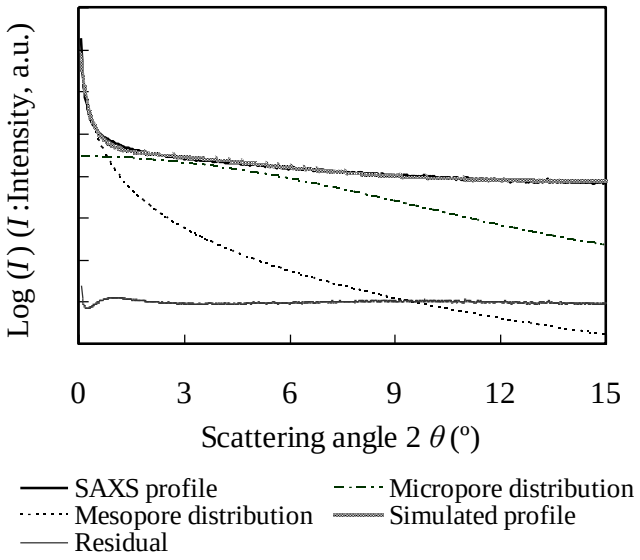

Figure 2. Analysis o pore distribution using NANO-Solver from a SAXS profile of HT2 charcoal which shows meso- and micropores in low and high degree region of 2. Micropore has the internal diameter less than 2 nm. Mesopore is that between 2 and 50 nm. The meaning of HT2 charcoal is referred to that in Table 1.

Table 2. BET Surface area and pore diameter analyzed by BJH model and by SAXS of HT1 and HT2 charcoals.

Charcoal	BET surface area (m^2/g)	BJH pore diameter (nm)	SAXS				
			Diameter of pore I (nm)	Vol. (%)	Diameter of pore II (nm)	Vol. (%)	Avr. Pore diameter (nm)
HT1	2.302	5.148	0.376	94.5	87.47	5.5	5.140
HT2	28.915	4.533	0.917	90.1	41.84	9.9	4.959

Note: The meaning of HT1 and HT2 is referred to that in Table 1. Pore I and II are referred to that in Fig. 2.

Table 2 lists the pore distribution, the volume fraction of pore and the average pore diameter of HT1 and HT2 charcoals measured by BJH method and analyzed by SAXS. The average pore diameter of HT1 and HT2 charcoals showed a minor difference and good agreement with that calculated by BJH method using N_2 adsorption analysis at 77 K (Barrett et al. 1951). On the other hand, wider distribution of mesopores was found in both HT1 and HT2 charcoals.

The size distribution of micropore in HT1 and HT2 charcoals are shown in Fig. 3. The average micropore size in HT1 charcoal was 0.376 nm which was smaller than that of 0.5 nm in the pine wood charcoal heat treated at 347ºC reported by Paris *et al*. (2005). The micropores were formed in HT1 charcoal when gas and tars evoluted up to 300ºC (Rodriguez-Reinoso and Molina-Sabio M 1992). In the case HT2 charcoal, the slope of SAXS profile increased slightly, equivalent to the greater diameter in the pores of 0.917 nm, which was greater than that of HT1 charcoal. The wider pore diameter with smaller distributions in HT2 charcoal was indicated by the slight increase in the SAXS signals. The heat treatments at 300ºC and followed by re-carbonization at 600ºC on HT2 charcoal released pyrolysis products which may influence on widening micropores already existed in the material. The micropore distribution of HT2 charcoal was smaller than that of HT1 charcoal, meaning that the widening of micropore might be occurred by connecting bigger pores leading to a certain pore size.

Figure 4a and c show the size distribution of micropore in HT1 charcoals in slow- and fast heating treatments. In slow heating treatment with additional $ZnCl_2$, lower scattering intensity of reaction time 120 and 180 min indicates lower porosity of the samples than that of 60 min. It is suggested that a prolonged reaction time from 60 min to 120 and 180 min caused the conversion of some micropore into wider pore sizes which reduced the porosity of the sample. The prolonged reaction time from 60 min to 120 min and 180 min also increased the diameter of micropore from 0.347 to 0.842 and 0.511 nm. In case of fast heating treatment, HT1 charcoals treated at different heating rates showed quite a similar scattering intensity which exhibited downward-convex profiles corresponding to a wide size distribution. The scattering intensity profiles of HT1 charcoals in fast heating treatment were lower than that in

slow heating treatment indicates lower porosity of the samples than that of HT1 charcoals in slow heating treatment.

Figure 4b and d show the size distribution of micropore in HT2 charcoals in slow- and fast heating treatments. In slow heating treatment, highest scattering intensity of reaction time 120 min and 180 min indicates higher porosity in the samples than that of 60 min. Heat treatment at 300ºC and then at 600ºC in the preparation HT2 charcoal may increase the release of volatile matters, resulting in widening micropore in the charcoal. Subsequent heat treatment at 700ºC for 120 and 180 min with additional $ZnCl_2$ enhanced the pores and created new micropore, which showed good agreement with the previous study (Lua *et al*. 2006) that reported the optimum temperature of carbonization at 600ºC for preparation of activated carbon. In the case of fast heating treatment, similar with previous discussion, the scattering intensity of samples was almost identical. The scattering intensity of HT2 charcoals in fast heating treatment was remarkable lower than that in slow heating treatment. However, fast heating treatment in a pulse current apparatus formed high distribution of homogeneous narrow micropore around 0.15-0.28 nm for HT1 charcoals and around 0.1 for HT2 charcoals which were different with an earlier investigation which reported that the fast heating produced macroporous carbon (Kurosaki *et al*. 2007).

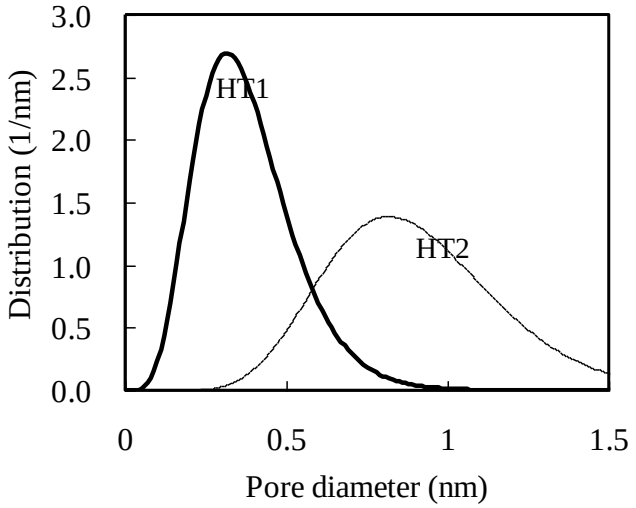

Fig. 3. Size distributions of micropores in HT1 and HT2 charcoals. The meaning of HT1 and HT2 is referred to that in Table 1.

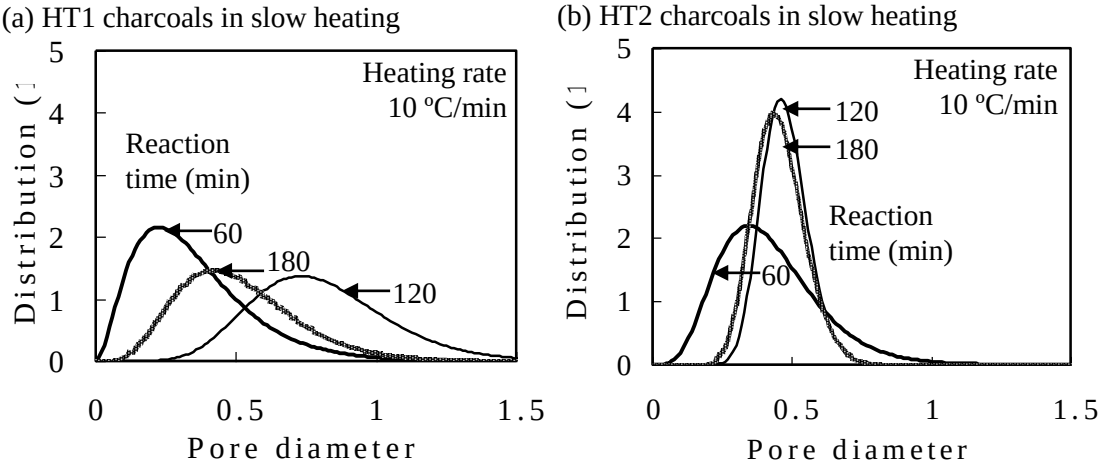

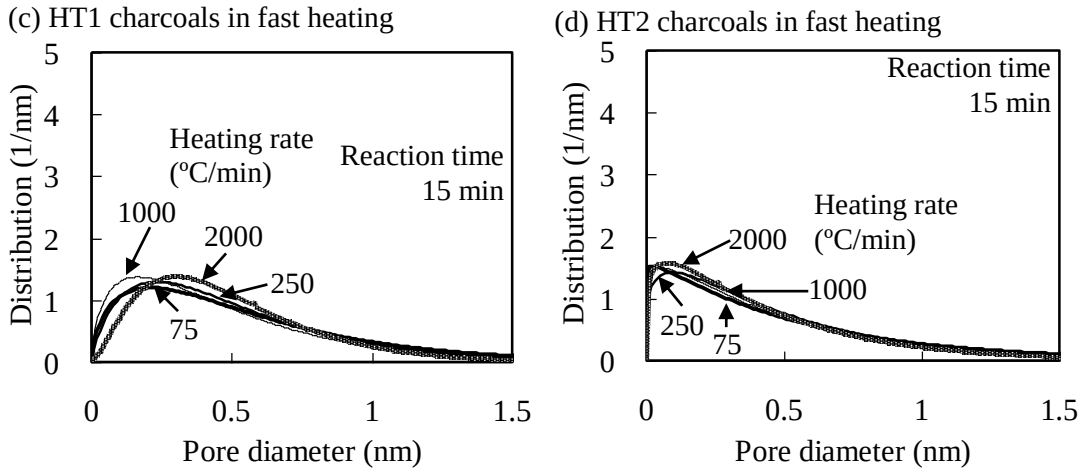

Figure 4. Size distributions of micropores in **a** HT1 and **b** HT2 charcoals heat-treated at 700ºC with heating rate 10ºC/min at different reaction times in slow heat treatment, in **c** HT1 and **d** HT2 chars heat-treated at 700ºC for 15 min at different heating rates in fast heating treatment. The meaning of HT1 and HT2 is referred to that in Table 1.

Surface Area

Surface area and adsorption isotherm were determined on HT2 charcoals in slow- and fast heating treatments due to the much different characteristics of micropore distribution. Figure 5a shows BET surface area of HT2 charcoals in slow heating treatment with additional $ZnCl_2$ in relationship to reaction time. HT2 charcoals prepared with reaction time 120 min and 180 min exhibited comparable BET surface area to the charcoal prepared with reaction time 60 min. The increasing porosity of HT2 charcoals in slow heating treatment due to the increasing reaction time from 60 min to 120 min and 180 min as shown by SAXS analysis was unable to be confirmed by gas adsorption analysis. A possible explanation is the closed porosity occurred in the charcoals prepared with reaction time 120 min and 180 min, which is not accessible for gas adsorption analysis.

Figure 5b shows BET surface area of HT2 charcoals in fast heating treatment in relationship to a heating rate. BET surface area of HT2 charcoals slightly increased with the increase of heating rate from 75 to 250ºC/min. Both BET surface area of HT2 charcoals prepared with heating rate 75 and 250ºC/min were comparable to HT2 charcoals in slow heating treatment. However, the increase of heating rate from 250 to 1000 and 2000ºC/min abruptly decreased BET surface area of HT2 charcoals with the value only 6.2 and 1.3 m^2/g, respectively. Fast heating may cause the surface of carbonized wood melted during the heat treatment with the rate of thousand degrees per minute (Diebold and Bridgwater 1997) which close or block the micropore which become inaccessible for gas adsorption analysis.

Figure 6a and b show the adsorption isotherm of HT2 charcoals in slow- and fast heating treatment. The shape of adsorption isotherms suggested that these charcoals exhibited Type I adsorption isotherms (Marsh and Rodriguez-Reinoso 2006) which containing microporosity only. Type I adsorption isotherm are typical of microporous solids in that micropore filling occurs significantly at relatively low partial pressure of < 0.1 P/P_o.[10]. HT2 charcoals in fast heating treatment prepared with reaction time 1000 and 2000ºC/min showed a low adsorption isotherm.

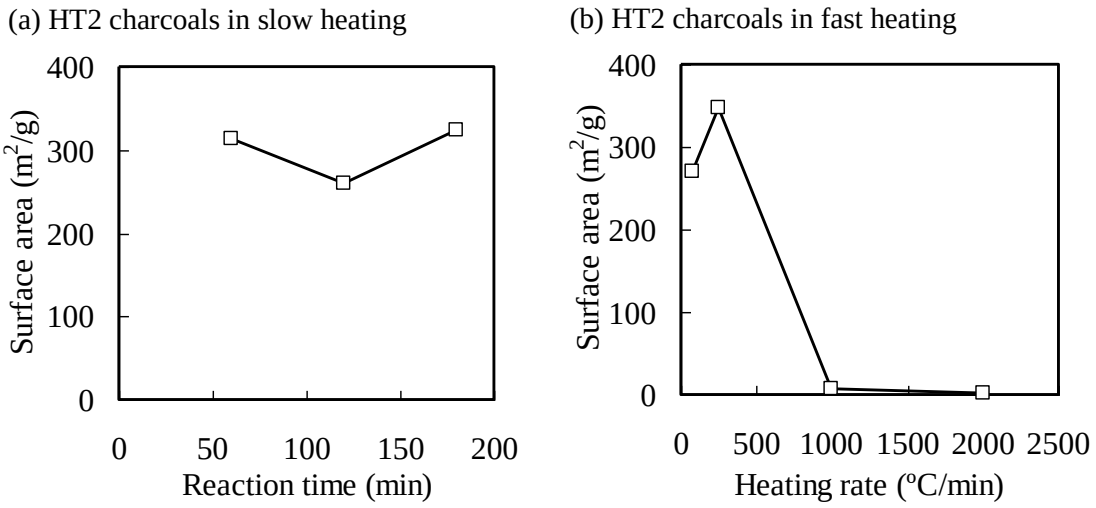

Figure 5. BET surface area of HT2 charcoals in **a** slow- and **b** fast heating treatment. The meaning of HT2 is referred to that in Table 1.

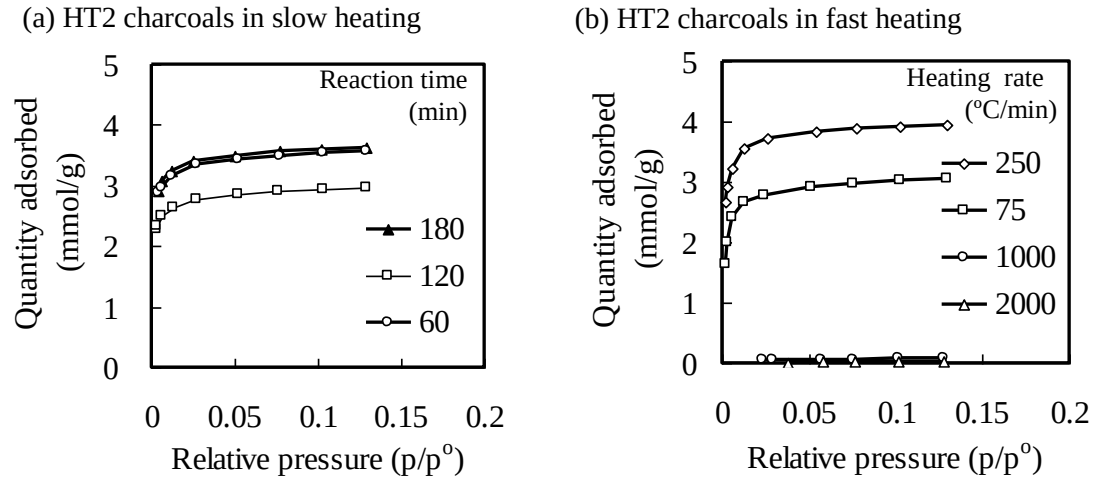

Figure 6. Adsorption isotherm of HT2 charcoals prepared by **a** slow- and **b** fast heating treatment. The meaning of HT2 is referred to that in Table 1.

Microstructural Change with Heat Treatments

Figure 7 shows the Raman spectra of HT1 and HT2 charcoals which exhibited D-band and G-band attributed to graphitic sp^2-bonded carbon. D-band is usually associated with the disordered structure of turbostratic carbon and G-band corresponds to the crystalline vibration (Ishimaru *et al.* 2007); Paris 2005). HT1 charcoal prepared from a heat treatment at 300ºC exhibited broad D-band and G-band with full width at half maximum (FWHM) of 279 and 125 cm^{-1}, respectively, corresponding to a typical of least ordered carbon material. The appearing of D-band and G-band on HT1 charcoal showed the aromatization occurred at heat treatment at 300ºC. HT2 charcoal prepared from a heat treatment at 300ºC and followed by re-carbonization at 600ºC showed narrowing D-band and G-band with FWHM of 206 and 82 cm^{-1} at positions shifted to 1362 and 1601, indicating the ordering of microstructure in the charcoal which was agreed with a previous study (Rodriguez-Reinoso and Molina-Sabio 1992) that reported the charcoal structure was consolidated at temperature range between 770-1120K. However the FWHM of D-band of HT2 charcoal was broader than that of carbonized wood reported previously (Yamauchi and Kurimoto Y 2003).

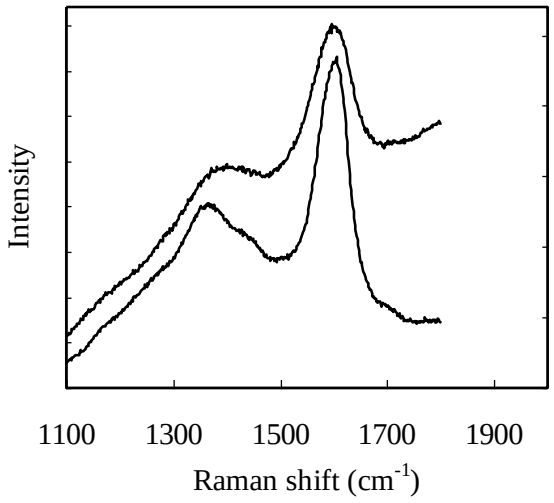

Figure 7. Raman spectra of HT1 and HT2 charcoals. The meaning of HT1 and HT2 is referred to that in Table 1.

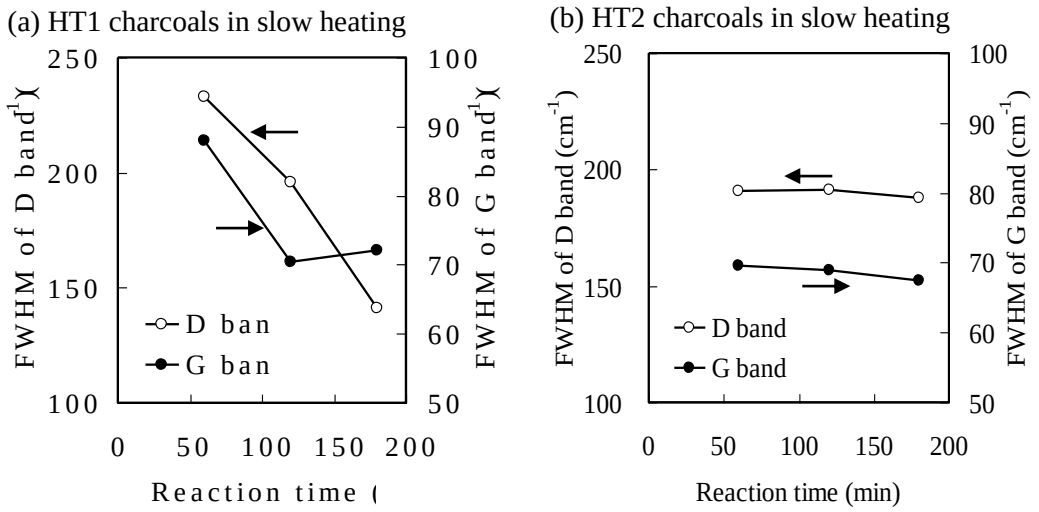

Figure 8. FWHM of D-band and G-band of **a** HT1 and **b** HT2 charcoals in slow heating treatment in relationship to reaction time. The meaning of HT1 and HT2 is referred to that in Table 1.

Effect of Slow Heating Treatment on Microstructural Change

Figure 8a and b show the plot of D-band and G-band width (FWHM) of HT1 and HT2 charcoals in slow heating treatment in relationship to reaction times. The FWHM of D-band and G-band of HT1 charcoals decreased with the increasing reaction time. The narrowing of band width suggests the structural arrangement or the ordering carbon element with the increase in reaction time (Yamauchi and Kurimoto Y 2003). The D-band and G-band of HT2 charcoals slow-heat-treated were narrower than that of HT1 charcoals slow-heat-treated for the reaction time of 60 and 120 min. It is suggested that re-carbonization at 600ºC, as second step of the slow heat treatment on HT2 charcoals contributed to the ordering microstructure. Prolonged reaction time of 180 min influenced significantly on the ordering of microstructure HT1 charcoal slow-heat-treated.

Effect of Fast Heating Treatment on Microstructural Change

The FWHM of D-band and G-band of HT1 and HT2 charcoals in fast-heating treatment in relationship to heating rates are shown in Fig. 9a and b. The FWHM of D-band and G-band of both HT1 and HT2 charcoals in fast heating

treatment became broader with the increasing heating rate. Meanwhile, HT1 charcoals fast-heat-treated showed broader D-band which indicated strong defects occurred compared with fast-heat-treated HT2 charcoals. As discussed on previously, fast heating treatment promotes the simultaneous chemical reactions including fragmentation and re-polymeration leading to a large formation of volatile matter (Kurosaki *et al*. 2003). HT1 charcoals released more intensively volatile matters during the fast heating treatment than that of HT2 charcoals. It is suggested that the fast volatilization contributed to more defects occurrence in the microstructure of HT1 charcoals. The defects in the microstructure of the charcoals intensively occurred with the increase of heating rate as shown by the broadening of the FWHM of D band. Therefore the fast heat treatments produced charcoal with lesser microstructural ordering than that of the slow heat treatments.

Figure 10a and b show the coherence length (L_a) of HT1 and HT2 charcoals in slow- and fast heating treatments, respectively. The L_a was reported to dependence on temperature with a decreasing trend with the increase of temperature (Paris 2005). In this study, L_a was insensitive to the increasing reaction time in slow heating treatments, as shown in Fig 10a and to the increasing heating rate in fast heating treatments, as shown in Fig 10b. HT1 and HT2 charcoals slow heat-treated at 10ºC/min up to 700ºC possessed higher L_a than that of HT1 and HT2 charcoals fast- heat-treated. It is suggested that the different chemical reaction occurred during the volatilization in the slow- and fast heating treatment as discussed previously may affect the growth of turbostratic crystallites

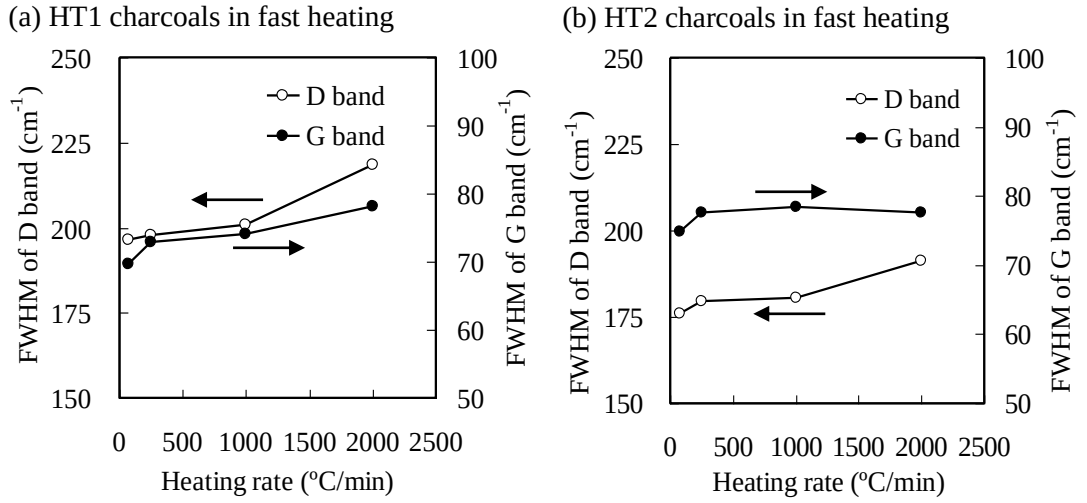

Figure 9. FWHM of D-band and G-band of **a** HT1 and **b** HT2 charcoals in fast heating treatment with the function of heating rate. The meaning of HT1 and HT2 is referred to that in Table 1.

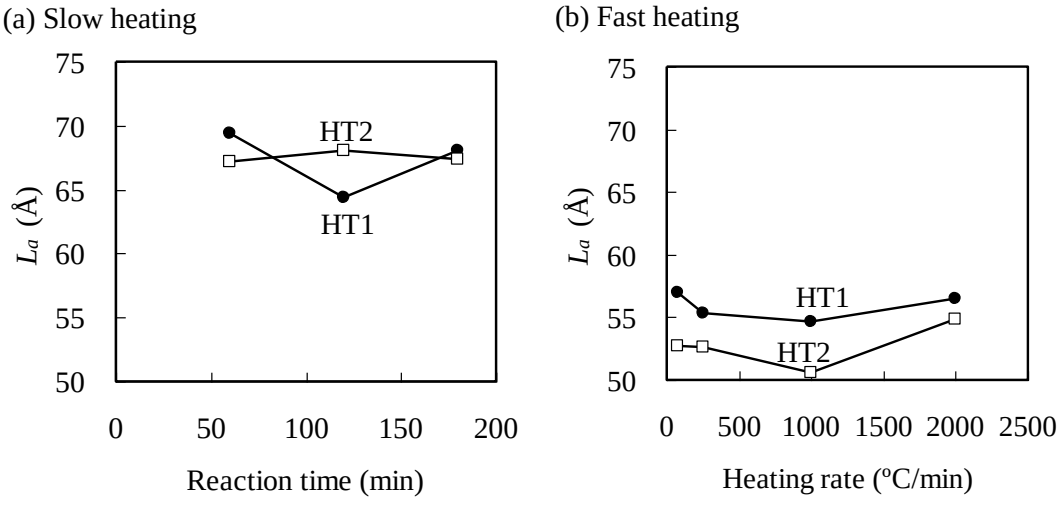

Figure 10. Coherence Length (L_a) of HT1 and HT2 charcoals **a** in slow- and **b** fast heat-treatment. *Filled circles*, HT1 chars; *empty squares*, HT2 chars. The meaning of HT1 and HT2 is referred to that in Table 1.

Conclusions

A slow heating treatment up to 700ºC on HT1 charcoal with the increasing reaction time for 120 and 180 min lead to the widening of micropore diameter without the opening new micropores indicating a reducing porosity and with the ordering microstructure comparing with those in HT1 charcoal with the reaction time for 60 min. Fast heating treatment on HT1 charcoal created micropore with narrower diameter and wider size distribution, but with lesser porosity and the disordering microstructure comparing with those in HT1 charcoal slow heat treated. In fast heating treatment on HT1 charcoal, the increase of heating rate produced charcoal with the decreasing micropore diameter and quite similar micropore size distribution, but with the disordering microstructure.

Re-carbonization at 600ºC in the preparation of HT2 charcoal contributed on the opening the new micropore with average diameter around 0.452-0.474 nm and on the ordering microstructure in the charcoals after the slow heat treatment up to 700ºC for 120 and 180 min. But some parts of the micropore in HT2 charcoal slow heat treated were inaccessible for N_2 gas. The increase of heating rate in fast heating treatment of HT2 charcoal was unchanged the distribution of micropore size and affected on the disordering microstructure. But BET surface area of HT2 charcoals slightly increased with the increase of heating rate from 75 to 250ºC/min then decreased with the increase of heating rate to 1000 and 2000ºC/min.

References

American Society for Testing and Materials. 1970. ASTM D 2867-70 Moisture in Activated Carbon.

American Society for Testing and Materials. 1970. ASTM D 2866-70 Total Ash Content of Activated Carbon.

American Society for Testing and Materials. 1977. ASTM D 1762-64 (Reapproved 1977) Chemical Analysis of Wood Charcoal.

Barrett, E.P.; L.G. Joyner; and P.P. Halenda. 1951. The Determination of Pore Volume and Area Distributions in Porous Substances I: Computational from Nitrogen Isotherms. J Am Chem Soc 73: 373-380.

Brunauer, S.; P.H. Emmett; and E. Teller. 1938. Adsorption of Gases in Multimolecular Layers. J Am Chem Soc 0: 309-319.

Demirbas, A. 2001. Carbonization Ranking of Selected Biomass for Charcoal, Liquid and Gaseous Products. Eng Convers and Management 42: 1229-1238.

Diebold, J.P. and A.V. Bridgwater. 1997. In: Bridgwater AV, Boocock DGB (Eds.) Development in Thermochemical Biomass Conversion, Vol. 1, Blackie Academic & Professional.

Fujisawa, M., T. Hata; P. Bronsveld; V. Castro; F. Tanaka; H. Kikuchi; T. Furuno; and Y. Imamura. 2004. SiC/C Composites Prepared from Wood-based Carbons by Pulse Current Sintering with SiO_2: Electrical and Thermal Properties. J Eur Ceram Soc 24: 3575-3580.

Greil, P. 2001. Biomorphous Ceramics from Lignocellulosics. J Eur Cer Soc 21: 105-118.

Ishimaru, K.; T. Hata; P. Bronsveld; and Y. Imamura Y. 2007. Microsectioning Study of Carbonized Wood after Cell Wall Sectioning. J Mater Sci 42: 2662-2668.

KE Hattula T.; U.M. Mrouch; and T. Luoma. 2001. Use of Liquid Smoke Flavouring as an Alternative to Traditional Flue Gas Smoking of Rainbow Trout Fillets (*Onchorhynchus mykiss*). Lebensm.-Wiss U-Technol 34: 521-525.

Kurosaki, F.; K. Ishimaru; T. Hata; P. Bronsveld; E. Kobayashi; and Y. Imamura. 2003. Microstructure of Wood Charcoal Prepared by Flash Heating. Carbon 41: 3057-3062.

Kurosaki, F.; H. Koyanaka; T. Hata; and Y. Imamura. 2007. Macroporus Carbon Prepared by Flash Heating of Sawdust. Carbon 45: 668-689.

Lua, A.C.; F.Y. Lau; and J. Guo. 2006. Influence of Pyrolysis Conditions on Pore Development of Oil-palm-shell Activated Carbons. J Anal Appl Pyrolysis 76: 96-102.

Mackay, D.M. and P.V. Roberts. 1981) The influence of pyrolysis conditions on yield and microporosity of lignocellulosic charcoals. Carbon 20: 95-104.

Marsh, H. and F. Rodriguez-Reinoso. 2006. Activated Carbon. Elsevier Ltd.

Paris, O.; C. Zollfrank; and G.A. Zickler. 2005. Decomposition and Carbonization of Wood Biopolymers-a Microstructural Study of Softwood Pyrolysis. Carbon 43: 53-66.

Pastor-Villegas, J.; C. Valenzuela-Calahorro; A. Bernalte-Garcia; and V. Gomez-Serrano. 1993. Characterization Study of Charcoal and Activated Carbon Prepared from Raw and Extracted Rockrose. Carbon 31: 1061-1069.

Rigaku Corporation. 2006. Cat. No. 9289H901/902 NANO-Solver (Ver3.4): Particle-/pore-size analysis software instruction manual. Manual No. ME13266A06, Sixth Edition. Japan.

Rodriguez-Reinoso, F. and M. Molina-Sabio. 1992. Activated Carbon from Lignocellulosic Materials by Chemical and/or Physical Activation: An Overview. Carbon 30: 1111-1118.

Tuinstra, F. and J.L. Koenig. 1970. Raman Spectrum of Graphite. J Chem Phys 53: 1126-1230.

Sulistyo, J.; T. Hata; H. Kitagawa; P. Bronsveld; M. Fujisawa; K. Hashimoto; and Y. Imamura. 2010. Electrical and Thermal Conductivities of Porous SiC/SiO_2/C Composites with Different Morphology from Carbonized Wood. J Mater Sci 45: 1107-1116.

Vyshnyakova, K.; G. Yushin; L. Pereselentseva; and Y. Gogotsi. 2006. Formation of Porous SiC Ceramics by Pyrolysis of Wood Impregnated with Silica. Intl J Appl Ceram Technol 3: 485-490.

Yamauchi, S. and Y. Kurimoto. 2003. Raman Spectroscopy Study on Pyrolyzed Wood and Bark of Japanese cedar: Temperature Dependence of Raman Parameters. J Wood Sci 49: 235-240.

Joko Sulistyo, Purnomo Darmadji and Sri Nugroho Marsoem
Faculty of Forestry, Universitas Gadjah Mada, Indonesia
Jl. Agro No. 1. Bulaksumur, Yogyakarta, Indonesia 55281
Tel : 62-274-6491428
Fax : 62-274-550541
E-mail : jsulistyo@ugm.ac.id

Toshimitsu Hata and Yuji Imamura (former)
Laboratory of Innovative Humano-habitability
Research Institute for Sustainable Humanosphere,
Kyoto University
Uji Campus, Gokasho, Uji, Kyoto 611-0011, Japan.
Tel. : +81-774-38-3601
Fax. : +81-774-38-3600
E-mail : hata@rish.kyoto-u.ac.jp

Anti-proliferative Activity of Some Oleanolic Acid Derivatives with Potent Topoisomerase Inhibitory Activity on B16 Melanoma Cells

Ahmed Ashour, Ryuichiro Kondo and Kuniyoshi Shimizu

Abstract

Our previous study included the semisynthetic reactions on oleanolic acid, a common wood-derived oleanane-type triterpene. Ten rationally designed derivatives of oleanolic acid were synthesized based on docking studies and tested for their topoisomerase I and IIα inhibitory activity. Semisynthetic reactions targeted C-3, C-12, C-13 and C-17. Some of these compounds act as dual inhibitors for both topoisomerase I and IIα giving new anticancer agents. The cytotoxic activity of these compounds on B16 melanoma cancer cells was evaluated. Results showed that most of these compounds have a higher cytotoxic activity on B16 melanoma cells.

Keywords: oleanolic acid, topoisomerase I and II, inhibitor, cytotoxic activity, B16 melanoma cells.

Introduction

Molecular modeling systems provide powerful tools for building, visualizing, analyzing, and storing models of complex molecular systems that can help interpret structure activity relationship (Cohen *et al*. 1990) where the techniques of combinatorial chemistry have revolutionized the development of active chemical leads where currently, instead of medicinal chemists making derivatives from scratch, a procedure is used whereby syntheses are based on combinatorial processes so that modification can be made in iterative fashion (Newman 2008). Over the past several years there has been a steadily evolving use of molecular modeling "computer-assisted drug design" as a tool in drug design.

Inhibition of topoisomerases is one of the important mechanisms of anticancer drugs (Pommier 2013). Pentacyclic triterpenes such as boswellic, betulinic, ursolic and oleanolic acids are reported to inhibit topoisomerases I and IIα by competing with DNA for topoisomerase binding through direct interaction with the enzyme preventing topoisomerase-DNA complex formation in both topoisomerases. Structure activity relationship suggested the general pentacyclic ring structure as important system for topoisomerase inhibitory activity. Carboxylation of the pentacyclic ring structure was also suggested to be necessary for topoisomerase inhibition (Syrovets *et al*. 2000). Based on these consequences, oleanolic acid which has been isolated from the unused parts of *Hibiscus sabdariffa* (Amer *et al*. 2011) was suggested as backbone for rational design of specific topoisomerase inhibitors.

In our previous study (Ashour *et al*. 2014), we have synthesized ten derivatives of oleanolic acid (Fig. 1) and tested for their inhibitory activity against topoisomerase enzymes. It was found that some compounds act as a dual inhibitor for both topoisomerase I and II. In this study, we have tested the activity of these compounds on B16 cells as an example for the cancer cells in an attempt to find the mechanism by which these compounds can inhibit the proliferation of these cells.

Materials and Methods

Plant Material

Oleanolic acid was isolated and purified from a methanolic extract of unused parts of *Hibiscus sabdariffa* grown in Egypt (Amer *et al*. 2011).

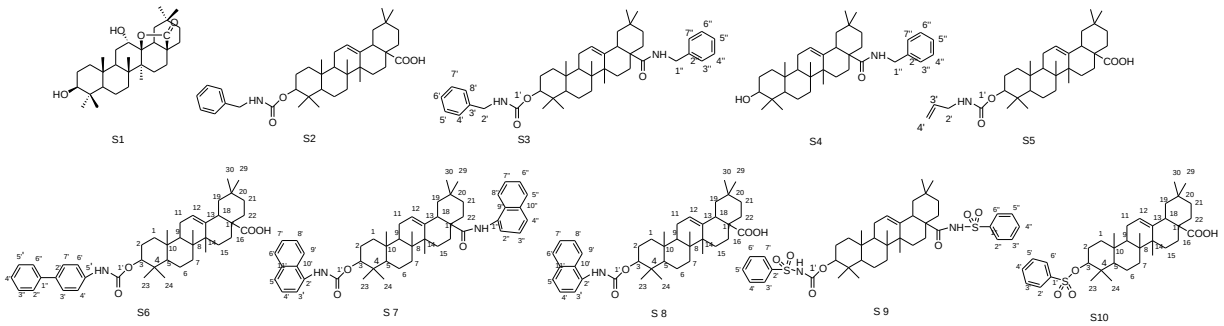

Figure 1. Structure of the synthesized compounds.

B16 Melanoma Cell Line Assay

This assay was determined as described previously (Arung *et al*. 2007). The cells were placed in two plates of 24-well plastic culture plates (one plate for determining melanin and the other for cell viability) at a density of 1 x 10^5 cells/well and incubated for 24 h in media prior to being treated with the samples. After 24 h, the media were replaced with 998 µL of fresh media and 2 µL of the test sample at maximum solubility (n = 3). At the same time, negative control (2 µL DMSO) and positive control; Arbutin at concentration 50 mg/mL in DMSO were tested. The cells were incubated for an additional 48 h, and then the medium was replaced with fresh medium containing each sample. After 24 h, the remaining adherent cells were assayed. To determine the melanin content (for one plate) after removing the medium and washing the cells with PBS, the cell pellet was dissolved in 1.0 mL of 1 N NaOH. After overnight keeping in dark, the crude cell extracts were assayed by using a microplate reader at 405 nm to determine the melanin content. The results from the cells treated with the test samples were analyzed as a percentage of the results from the control culture. On the other hand, cell viability was determined by using MTT assay which provides a quantitative measure of the number of viable cells by determining the amount of formazan crystals produced by metabolic activity in treated versus control cells. So, for the other well plate, 50 µL of MTT reagent in PBS (5 mg/mL) was added to each well. The plates were incubated in a humidified atmosphere of 5% of CO_2 at 37°C for 4 h. After the medium was removed, 1.0 mL isopropyl alcohol (containing 0.04 N HCl) was added, and the absorbance was measured at 570 nm after overnight keeping in dark.

Results and Discussion

B16 Melanoma Cell Biological Activity

B16 melanoma cells have been known to produce melanin pigment. To understand the mode of action of oleanolic acid derivatives against cells, their effects on melanin production and cell growth of B16 melanoma cells have been evaluated. From the results of B16 melanoma cell assay (Fig. 2), it was found that Compounds S5, S9 and S10 have a high cytotoxic activity. These compounds may inhibit the growth of the cancer cells through inhibition of topoisomerase enzyme as we have reported the high inhibitory activity of these compounds against topoisomerases in our previous study (Ashour *et al*. 2014) or through their cytotoxic effect caused by other mechanisms. However we have also found that compounds S1, S3, S4 and S7 also have good melanin biosynthesis inhibitory activity in B16 melanoma cells with less cytotoxic activity. It means these compounds (S1, S3, S4 and S7) inhibit the function of the cancer cells such as melanin biosynthesis by a mechanism other than the cytotoxicity. The investigation for clarifying the precise mode of action of them are under investigation.

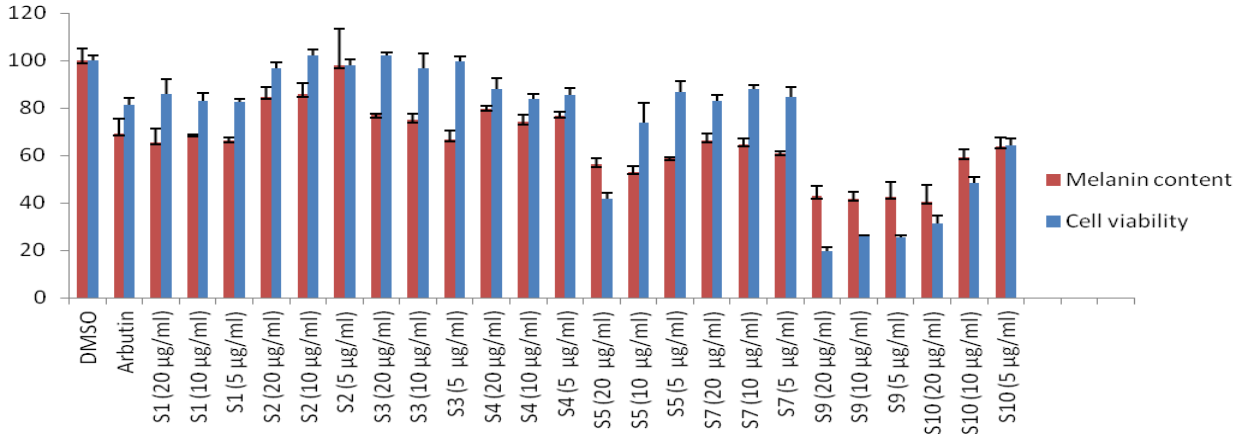

Figure 2. Effect of compounds on melanin formation in B16 melanoma cell. The values are represented as the mean ± standard deviation (SD), n=3. Significant difference from the control value and each compound was determined by Student's t-test: **P* < 0.05, ***P* < 0.01.

Reference

Amer, M.; S. El-Sharkawy; A. Marzouk; and A. Ashour. 2011. Chemical Constituents of Corncobs. J. of Environ. Sci. 40: 251-258.

Arung, E.; K. Shimizu; and R. Kondo. 2007. Structure Activity Relationship of Phenyl Substituted Polyphenols from *Artocarpus heterophyllus* as Inhibitors of Melanin Biosynthesis in Cultured Melanoma Cell. Chemistry & Biodiversity 4: 2166-2171.

Ashour, A.; S. El-Sharkawy; M. Amer; F. Abdel Bar; Y. Katakura; T. Miyamoto; N. Toyota; T. Hai Bang; R. Kondo; and K. Shimizu. 2014. Rational Design and Synthesis of Topoisomerase I and II Inhibitors Based on Oleanolic Acid Moiety for New Anti-cancer Drugs. Bioorganic and Medicinal Chemistry 22(1): 211-220.

Cohen, N.; J. Blaney; C. Humblet; P. Gund; D. Barry. 1990. Molecular Modeling Software and Methods for Medicinal Chemistry. J. Med. Chem. 33: 584-594.

Newman, D. 2008. Natural Products as Leads to Potential Drugs: An Old Process or the New Hope for Drug Discovery. J. Med. Chem. 51: 2589-2599.

Pommier, Y. 2013. Drugging Topoisomerases: Lessons and Challenges. ACS Chemical Biology 8: 82-95.

Syrovets, T.; B. Büchele; E. Gedig; R. Slupsky; T. Simmet. 2000. Acetyl-Boswellic acids are Novel Catalytic Inhibitors of Human Topoisomerases I and IIα. Mol. Pharmacol. 58: 71-81.

Ahmed Ashour
Department of Pharmacognosy, Faculty of Pharmacy,
Mansoura University, Mansoura, Egypt
Tel : 002-01001737941
E-mail : ahmedadelashour@yahoo.com

Ryuichiro Kondo
Department of Agro-environmental Sciences,
Faculty of Agriculture, Kyushu University, Fukuoka, Japan
E-mail : ryukondo@agr.kyushu-u.ac.jp

Kuniyoshi Shimizu
Department of Agro-environmental Sciences,
Faculty of Agriculture, Kyushu University, Fukuoka, Japan
Tel/Fax : 092-642-3002
E-mail : shimizu@agr.kyushu-u.ac.jp

Volume 9, Number 1, April 2018 ISSN 2087-3840

WOOD RESEARCH Journal

Journal of Indonesian Wood Research Society

Annals of the Wood Research Journal

Wood Research Journal is the official journal of the Indonesian Wood Research Society. This journal is an international medium in exchanging, sharing and discussing the science and technology of wood.

Aims and Scope

The journal publishes original manuscripts of basic and applied research of wood science and technology related to Anatomy, Properties, Quality Enhancement, Machining, Engineering and Constructions, Panel and Composites, Entomology and Preservation, Chemistry, Non Wood Forest Products, Pulp and Papers, Biomass Energy, and Biotechnology. Besides that, this journal also publishes review manuscripts which topics are decided by the Editors.

Imprint

WRJ is published by Indonesian Wood Research Society
ISSN print: 2087-3840
Electronic edition is available at:
http://ejournalmapeki.org/index.php/wrj

Publication Frequency

Journal is published in one volume of two issues per year (April and October).

Peer Review Policy

WRJ reviewing policies are: Every submitted paper will be reviewed by at least two peer reviewers. Reviewing process will consider novelty, objectivity, method, scientific impact, conclusion and references.

General Remarks

Manuscripts will be accepted for publications are those discussing and containing results of research on wood science and technology, and reviews on specific topics, which are decided by the Editors and have not been published elsewhere. Authors are requested to correct the manuscripts accepted for publications as suggested by the Reviewers. Editors could change positions of Figures and Tables.

Manuscripts Preparations

1. Manuscripts must be in English, typewritten using Word, Arial Narrow, single space, 3 cm of left and right margin and 2.5 cm of top and bottom margin of a Letter paper size. Title is printed with a font size of 14 pt, Authors are of 12 pt, and Text is of 10 pt.
2. Manuscripts should be checked for spelling and grammar by a native speaker.
3. Manuscripts compositions:

3.1. Title
3.2. Complete name of Authors
3.3. Abstract
3.4. Key words
3.5. Texts:
Introduction
Materials and Methods
Results and Discussion
Conclusions (and Suggestions)
References
Name and complete address of Authors
Appendix

4. Other rules:

4.1. Names of wood are followed by Botanical Name.
4.2. Values between are written using this symbol (□), e.g. 3.75 □ 8.92%.
4.3. Editors could modify Figures without changing their substantial meaning.
4.4. References are arranged from A to Z.
4.5. References in text are written as this example: (Palomar *et al.* 1990; Arancon 1997).
4.6. Examples of writing of References: Altschul, S.F.; T.L. Madden; A.A. Schäffer; J. Zhang; Z. Zhang; W. Miller; D.J. Lipman. 1997. Gapped BLAST and PSI-BLAST: A New Generation of Protein Database Search Programs. Nucleic Acids Res. 25: 3389-3402.

Editorial Address

Research Center for Biomaterials,
Indonesian Institute of Sciences
Jl. Raya Bogor Km 46, Cibinong,
Bogor 16911, Indonesia
Tel/Fax : +62-21-87914511/87914510
E-mail : mapeki.wrj@gmail.com
Web-site : www.ejournalmapeki.org

Volume 9, Number 1, April 2018 ISSN 2087-3840

WOOD RESEARCH Journal

Journal of Indonesian Wood Research Society

Example of Table and Figure

Table 1. Effects of temperature on *in vitro* growth of seedlings.

Temp. (°C)	Shoot length (mm)	Number of leaf	Fresh weight (g)
25	59.2 ± 10.6[c]	4.5 ± 0.8[a]	0.29 ± 0.13[a]
27	88.5 ± 9.3[a]	4.8 ± 0.9[a]	0.40 ± 0.12[a]
29	75.0 ± 11.1[b]	3.8 ± 0.6[a]	0.30 ± 0.07[a]

Note: Values (average ± standard deviation) with different letters are statistically significant according to Tukey's multiple comparison test. Data were recorded after 4 weeks of culture. MS medium was used as a basal medium without any PGRs. Number of sample = 10.

Source: Chujo *et al* 2010.

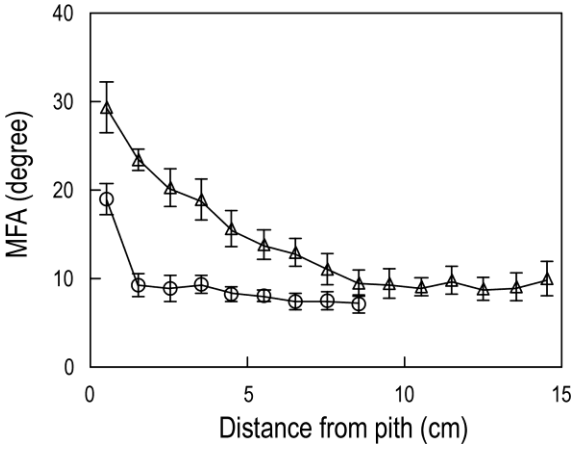

Figure 3. Radial variation of microfibril angle of the S2 layer in tracheid. Open circle, *Agathis* sp.; open triangle, *Pinus insularis*; Bars indicate the standard deviation. (Source: Ishiguri *et al* 2010)


9 772087 384007